Winter 2022

Predator-induced Hatching Plasticity of Northeastern Pacific Coast Nudibranchs

Geoffrey Masato Mayhew
Western Washington University, geoffmmayhew@gmail.com

Predator-induced Hatching Plasticity of Northeastern Pacific Coast Nudibranchs

By

Geoffrey Masato Mayhew

Accepted in Partial Completion
of the Requirements for the Degree
Master of Science

ADVISORY COMMITTEE

Dr. Benjamin Miner, Chair

Dr. John Lund

Dr. Brian Bingham

Dr. Shawn Arellano

GRADUATE SCHOOL

David L. Patrick, Dean

Master's Thesis

In presenting this thesis in partial fulfillment of the requirements for a master's degree at Western Washington University, I grant to Western Washington University the non-exclusive royalty-free right to archive, reproduce, distribute, and display the thesis in any and all forms, including electronic format, via any digital library mechanisms maintained by WWU.

I represent and warrant this is my original work, and does not infringe or violate any rights of others. I warrant that I have obtained written permissions from the owner of any third party copyrighted material included in these files.

I acknowledge that I retain ownership rights to the copyright of this work, including but not limited to the right to use all or part of this work in future works, such as articles or books.

Library users are granted permission for individual, research and non-commercial reproduction of this work for educational purposes only. Any further digital posting of this document requires specific permission from the author.

Any copying or publication of this thesis for commercial purposes, or for financial gain, is not allowed without my written permission.

Geoffrey Masato Mayhew

14 March 2022

Predator-induced Hatching Plasticity of Northeastern Pacific Coast Nudibranchs

A Thesis
Presented to
The Faculty of
Western Washington University

In Partial Fulfillment
Of the Requirements for the Degree
Master of Science

by
Geoffrey Masato Mayhew
March 2022

Abstract

Many organisms have complex life cycles that include ontogenetic niche shifts, or changes to morphology, physiology, diet, predators, and habitat. Natural selection favors individuals that choose the optimal time to undergo ontogenetic niche shifts that avoids unnecessary losses to fitness, and niche shift timing is therefore considered a plastic trait. Hatching is a common niche shift within animals, and modifications to hatch timing can mediate the costs and benefits of hatching sooner or later, depending on varying predation risk, resource availability, or habitat conditions. Predator-induced hatching plasticity in particular is well-documented within amphibians as well as other terrestrial vertebrates and arthropods, but few cases have been documented in the marine environment. This is likely due to the difficulty of making observations of hatching activity, as many marine invertebrates hatch as near-microscopic larvae. The purpose of this study was to develop hatching detectors that improve the ease and frequency of observations of hatching and then demonstrate their utility in investigations of hatching plasticity of two nudibranch species. The hatching detectors, comprised of an array of paired infrared emitters and phototransistors, measure fluctuations in absorbed infrared light to detect hatching. Coupled with wireless transmissions of hatching data, these sensors allowed quasi-real-time monitoring of hatching activity and high-temporal resolution estimates of hatch timing with minimal disturbance to developing embryos. Using these hatching detectors, I wanted to examine whether the nudibranchs *H. crassicornis* and *O. bilamellata* exhibit hatch timing plasticity. Given their benthic development within embryo masses and planktonic development after hatching, I hypothesized that both species would accelerate hatch timing when their embryo masses were presented with predation cues from

benthic predators. I first investigated hatching plasticity in the aeolid *H. crassicornis* in response to a simulated predator attack (disruption of the embryo mass outer envelope at age 7 d) and to chemical cues from the embryo predator *Heptacarpus brevirostris* and the non-predator *Petrolisthes eriomerus* in a fully-crossed experimental design. There was an apparent interaction between the mechanical cue and embryo mass batch where the simulated predator attack had no effect on the first batch of embryo masses but reduced time-to-hatching in the second batch of embryo masses. The chemical cue had no significant effect on hatch timing. I performed another experiment with the dorid *O. bilamellata* to determine if they modify hatch timing in response to chemical cues from the embryo predator *H. brevirostris* or the non-predator *Nucella lamellosa*, but also found no significant effect. Although this study did not find clear evidence of predator-induced hatching plasticity in these two nudibranchs species, the hatching detectors functioned as intended and provide a means to facilitate future examinations of hatching plasticity in animals with similar life histories.

Acknowledgements

I would like to give massive thanks to my thesis advisor, Dr. Ben Miner, for his guidance and boundless enthusiasm throughout my years in undergraduate and graduate school. My career in data analysis can largely be credited to him, as he introduced me to R. Huge thanks go to my thesis committee as well: Dr. Brian Bingham, Dr. Shawn Arellano, and Dr. John Lund. Dr. Lund was incredibly generous with his time and materials in the development of the hatching detectors.

Thank you to Peter Thut and the rest of the staff of the Biology Department stockroom. Whether it was salinity refractometers, airline tubing, or vacuum filters and desiccators, I could always count on your assistance to fabricobble and maintain my experiments. I also want to give a shoutout to Reza Afshari for his assistance in the assembly of the hatching detector circuitry and keeping the 3-D printers running around the clock.

My research would not have been possible without the help of a squad undergraduate research assistants: Mia Lints, Charlie Hauser, Elliot Tan, Claire Fink, Tessa Beaver, Spencer Edwards, and Alexander Ward. Thank you all so much for collecting critters and making observations at strange hours of the day, spending hours filtering and changing water, and everything else to keep the experiments going. Additional kudos to Tessa for maintaining the *Onchidoris* experiment while I started my job in Seattle, as well as for helping me defend the lab from a nearly catastrophic flood!

Thank you to the Thon Family for the summer fellowship and the Graduate Research Review Committee for providing essential funding of my thesis. Thank you to the Biology Department for providing the teaching assistantships towards my tuition waiver and living stipend.

I would also like to acknowledge my former colleagues at the Washington State Department of Natural Resources for supporting my return to school, as well as my current colleagues at the Alaska Fisheries Science Center for providing me the time to complete my thesis.

Finally, I want to thank my friends and family. Thank you, my fellow biology graduate students, especially to my buds Christina Kohnert, Matt McTernan, and Zoe Zilz. My parents Doug and Yasuko Mayhew fostered my passion for science and instilled the work ethic required to pursue my dreams. Thank you Taizo and Kazue Kato, my Ojiichan and Obaachan, for your tremendous financial support and for inspiring me to craft and work with my hands. Thank you Michael and Dianne Murphy, the world's best in-laws, for your endless support. Thank you Kylo and Evie for the cat antics, and to Boris the tortoise for literally being there since middle school. Lastly, I give infinite thanks to my wife Natalie. I definitely could not have done this without your support, patience, and love.

Table of Contents

List of Tables

List of Figures

Chapter 1: Background and Overview

Phenotypic Plasticity

Phenotypic plasticity is the capacity for an organism to exhibit a range of phenotypes in response to changes to the environment. This plasticity is not always adaptive, but if an organism can effectively match its phenotype to its variable environment, it can improve survival and avoid reductions to fitness caused by mismatches (Whitman & Agrawal 2009). Plastic responses are ubiquitous and can manifest in many ways: morphologically, biochemically, behaviorally, developmentally, and physiologically (Adler & Harvell 1990, Strathmann 1993, Whitman & Agrawal 2009), might be continuous, graded or discrete, and reversible or irreversible. Similarly, plastic responses have a variety of inducers both abiotic and biotic (e.g., changes to temperature, salinity, or wave action, food availability, or threat of predation) (West-Eberhard 1989, Whitman & Agrawal 2009).

Phenotypic plasticity serves an important role in adaptive evolution as it allows individuals to respond to environmental variation in real time compared to fixed traits that are selected over generations when the environmental variation occurs over coarser time scales. Traditional evolutionary theory is centered on a population's capacity to adapt by utilizing the population's variety of genotypes to produce a variety of phenotypes upon which natural selection acts. However, phenotypic plasticity expands upon this paradigm as a mechanism through which a single genotype can express multiple phenotypes (oftentimes achieved through differential gene expression) and is itself a trait upon which selection acts (West-Eberhard 1989). Variable environments therefore support the accumulation of novel yet cryptic genetic variants necessary for speciation (Pfennig et al. 2010).

It is important to consider the costs and constraints of phenotypic plasticity as no organism can produce the optimal phenotype in all environments. Indeed, in a homogenous

environment, fixed organisms have an advantage over plastic organisms as there is an inherent cost for the ability to be plastic such as additional structures to sense and process environmental changes and regulatory mechanisms to invoke plastic responses (Scheiner 1993, DeWitt et al. 1998). Plastic responses have energetic trade-offs as well, such as through the production of defensive structures at the cost of lower growth and fecundity (Harvell 1986, Hoverman et al. 2005). Plasticity also comes with the risk of incorrectly interpreting environmental cues or not inducing plastic responses quickly enough to track environmental changes, resulting in poor energetic investment or lost opportunities to feed, grow, or reproduce (Warkentin 2005). Similarly, the degree to which plastic responses are reversible also influences the potential costs (Orizaola et al. 2012). Thus, phenotypic plasticity benefits individuals that accurately respond to (and even predict) changes in their environments when the benefits outweigh the costs (Harvell 1990, Warkentin 2011).

Plasticity in timing of ontogenetic niche shifts

Many organisms have complex life cycles that include changes to morphology, physiology, diet, predators, and habitat. Such changes can be rapid, as in metamorphosis within many amphibians (Warkentin 1995) or germination within plants (Donohue 2002), or gradual, as in the case of an alligator that progresses from preying on insects to crustaceans to larger vertebrates (Subalusky et al. 2009). Such changes, labeled ontogenetic niche shifts, are typically irreversible and alter an organism's role in its environment, including its interactions with its population, community, and environment (Werner and Gilliam 1984). Also, by utilizing different resources at different life stages, a population can reduce intraspecific competition (Rudolf & Rasumussen 2013) and mediate predation risk (Kimirei et al. 2013).

The timing of niche shifts can have large impacts on an organism's growth, survival and fitness. For example, the timing of adult salmon migration to freshwater bodies affects their survival (e.g., temperature and predation), and the timing of their spawning affects the timing of the emergence of their offspring, whose survival depends on availability of food and avoiding predators (Quinn et al. 2002, Lisi et al. 2013). Similarly, the timing of germination in *Arabidopsis thaliana* affects overwintering survival, size at reproduction, and fruit production (Donohue 2002). Natural selection favors individuals that choose the optimal time to undergo ontogenetic niche shifts that avoids unnecessary losses to fitness. Niche shift timing is therefore considered a plastic trait that evolves over time.

Within many animal groups, hatching is perhaps the earliest ontogenetic niche shift and represents the period when an individual gains mobility and access to new resources. The positive correlation between temperature and development, and therefore hatch timing, is straightforward, but hatch timing may also be a function of food or host availability, salinity or oxygen, or chemical cues from conspecifics (Warkentin 2011). The effects of predation risk are more complex (Benard 2004). Both eggs and hatchlings are subject to high predation risk, but it can be mediated by hatching earlier or later depending on whether habitats and predators differ between life stages. Predator-induced hatching plasticity (PIHP) in amphibians is well-documented (Sih & Moore 1993, Warkentin 1995, Warkentin 2005, Vonesh 2005, Touchon et al. 2006, Smith and Fortune 2009), with most other cases in freshwater and terrestrial environments and a few cases in the marine environments (Miner 2010, Strathmann 2010).

Within most of the literature on hatching plasticity, the detection of hatching was relatively straightforward because hatching could be easily observed by the naked eye. The eggs of the red-eyed tree frog *Agalchnis callidryas* are approximately 5.2 mm prior to hatching

(Warkentin 2002) and the emerging tadpoles are easily spotted as their wriggle from their eggs. Hatchlings of the spitting spider *Scytodes pallida* are smaller but still visible without aid, between 0.6-0.8 mm (Li 2002). Hatchlings of the marine whelk *Nucella lamellosa* are similarly sized at approximately 0.85 mm (Miner 2010), but hatching is easily observed when the plug at the tip of egg capsules detaches to allow juveniles to crawl out. The hatchlings of the polychaete *Boccardia proboscidea* are small (200-300 µm, Gibson 1997), but hatching is easily observed because it is facilitated by a brooding mother that tears open each capsule. In all these cases, hatching events can be identified at the level of individual hatchlings or the egg structures. However, observing hatching events is more problematic for species with smaller hatchlings that do not have extraembryonic structures or other traits that conveniently indicate hatching. Such is the case for many marine invertebrates, which likely contributes to the lack of hatching plasticity studies for this group.

Observing hatching in nudibranchs is particularly difficult. Many nudibranch species have small egg capsules between 80-160 µm (Hurst 1967) and the hatched planktonic veliger larvae are inconspicuous, especially when larvae are in low concentrations. In a laboratory setting, backlighting a small container helps as it illuminates the veligers, but care and/or experience is still required to not mistake bubbles, debris, or other plankton species as nudibranch larvae. The egg masses become more translucent as hatching progresses from the edges towards the center of the egg mass, but it is difficult to detect the time of first hatching using this method. Moreover, egg masses oftentimes have sections that are devoid of eggs, so observations of changes in the transparency of the egg mass must be made carefully. Hatching is easily observed with the aid of a microscope, but this is not only tedious and time consuming,

but can also introduce mechanical disturbances, temperature changes, or disruptions to light cycles that affect time-to-hatching and increase the variance of estimates.

The complexity and potential risk of disturbing nudibranch embryo masses while making observations of hatching activity might also limit the frequency at which observations can be made. The burden of the frequency of observations is amplified by the number of replicates, so experimenters must manage the tradeoffs between the frequency of observations with the total number of replicates (i.e., statistical power). More observations results in higher risk of disturbance that can lead to greater variability in measurements of hatching timing. In other hatching plasticity studies, the frequency of observations for hatching varied, such as a few times per day (Warkentin 1995, Strathmann et al. 2010), on a daily basis (Smith & Fortune 2009), or every two days (Vonesh 2005, Miner 2010). Without less-invasive methods of assessing hatching in nudibranch egg masses, one must weigh the risks of disturbing incubation against the time and effort required for a thorough assessment of each sample, all within the context of the constraints of the sample size and the time required to collect all measurements.

Studies of hatching plasticity in marine invertebrates would greatly benefit from methods that automate observations of hatching activity with minimal disturbance. Such methods would enable experimenters to increase sample sizes to improve statistical power as well as increase the frequency of observations. This not only improves the temporal resolution of time-to-hatching estimates to detect smaller effect sizes, but also broadens the types of questions that can be investigated. For instance, the embryos within an embryo mass do not always hatch in a synchronized manner (Pechenik 1990, Avila 1998), and high-resolution measurements of hatching activity could characterize the overall duration of hatching and whether it is unimodal or multimodal. In an effort to address many of the difficulties of observing hatch timing in near-

microscopic organisms that hatch from benthic embryo masses, such as nudibranchs, I designed hatching detectors that largely automate measures of hatching activity. Moreover, these sensors were designed to be deployed within larger aquaria to which experimental treatments can be assigned. I will present the construction and function of these hatching detectors in Chapter 2. In Chapter 3, I will demonstrate the application of these hatching detectors to investigate whether embryos of the aeolid nudibranch *Hermissenda crassicornis* and the dorid nudibranch *Onchidoris bilamellata* exhibit PIHP in response to mechanical and/or chemical cues.

Chapter 2: Hatching Detectors

Improved tools for monitoring hatching activity of swimming planktonic larvae from benthic egg masses will improve the ability to survey plastic hatching responses within invertebrates. The tools and methods described here were developed particularly for Northeast Pacific nudibranch species, but can be applied generally to other species with similar life histories. These methods were developed with several intentions in mind: to maximize its utility within various experimental designs, to minimize disturbances to the study subjects, to reduce observation error, to improve the temporal resolution of hatch timing estimates, to streamline the husbandry of study specimens, and to improve sample sizes. Most PIHP studies focus on one hatching cue (exception of Tollrian & Laforsch 2006 who crossed predator kairomones and turbulence on *Daphnia* shells), so the hatching detectors were designed with the potential to test chemical and mechanical cues simultaneously.

To investigate PIHP in Northeast Pacific nudibranchs, I developed customized sensors and software to allow near real-time monitoring of hatching activity and provide high-temporal resolution estimates of hatch timing. Each nudibranch egg mass was placed in a hatching detector with infrared light hatching sensors located above it to monitor the activity of hatched veliger larvae. These hatching detectors had mesh sides so that water was shared with a larger aquarium. This exposed the incubating egg masses to chemical cues from potential predators or non-predators residing in the larger aquarium, while also excluding those specimens from disturbing the egg mass or interfering with the measurements of the sensors. These aquaria were maintained in a water table circulating refrigerated fresh water, and an automatic water change system was constructed to simplify aquaria maintenance and minimize disturbances to the egg masses and sensors.

To my understanding, no other studies have utilized infrared light to detect hatching activity. Cronin & Forward (1986) used an infrared light to backlight a 1.9 m tall column and recorded each 10-cm section with an IR-sensitive film to track the vertical migration of crab zoea larvae in response to current, tidal, and light cycles. The crab larvae absorbed or reflected enough IR light to allow researchers to count individual larvae and indicates that planktonic invertebrates in that size range can occlude enough infrared light to be detected by sensors.

Hatching Detectors

The hatching detectors were developed over roughly two years. Considerable prototyping and testing with different electrical components, materials, and designs were required to arrive at the configuration that was used in my study. In my description of these sensors, I will highlight the most important details of their construction and design considerations. For the sake of brevity I will not describe earlier sensor designs, most of which had inadequate waterproofing or sensitivity.

The frames of the hatching detectors (Figure 2.1) were constructed from 7.5 cm x 7.5 cm x 10 cm polycarbonate vessels (Magenta GA-7 vessels from Carolina Biological Supply Company). Two 4.5 cm x 2.5 cm rectangles were cut from two opposing sides, 20 mm above the bottom of the vessel, and both were covered with 60 µm nylon mesh using hot glue. This mesh size was selected because the minimum diameter of the oocytes and veliger larvae of local nudibranch species is approximately 100 µm (Strathmann 1987) and accounted for the length of the diagonals of the mesh as approximately 85 µm. The vessels were covered by polypropylene lids to minimize contamination and prevent splashing water from disturbing measurements by

the sensors, and a small hole was drilled into the lids to prevent a vacuum that would impair water flow through the nylon mesh and the enclosing aquaria.

Each hatching detector had an array of six paired infrared light emitters and phototransistors situated 5.5 cm above the bottom of vessel. Swimming planktonic larvae that hatch from benthic egg masses oftentimes exhibit positive phototaxis (Miller & Hadfield 1986) and therefore swim upwards. This would take them through the sensor arrays and cause variations in the IR intensity received by the phototransistors. In my observations, hatched nudibranch larvae typically swam erratically throughout the water column within the hatching detectors. IR light was used due to its high absorption in water to prevent neighboring sensors from receiving light from other sensors and because the long wavelength is beyond the sensitivity of most marine organisms (McCormick et al. 2019). The sensor arrays were comprised of a circuit on two separate boards situated on opposite sides of each hatching detector. The main board was connected to a power supply, had six phototransistors spaced equally along the length of the board, and a wireless transmitter. A ribbon cable extended from the main board to power six IR emitting LEDs on the second board. An Atmel Mega microcontroller on the main board was programmed to turn on each IR emitter/phototransistor pair sequentially, calculate exponentially weighted moving average and exponentially weighted moving variance of the magnitude of IR light intensity in arbitrary units, and regularly transmit information to a nearby workstation (Appendix A, Appendix B). In essence, when hatched larvae pass between the IR emitter/phototransistor pairs, the measured intensity of IR light fluctuates. As more larvae hatch, the variation in measured IR light increases, and the time of hatch timing is interpreted as sustained departure from background measurements.

Sleeves were 3-D printed out of black ABS plastic to align the IR emitters/phototransistors of the boards on opposite sides of the polycarbonate vessels. The sleeves had built-in pinholes in front of the phototransistors to ensure that each phototransistor only received IR light from its paired emitters and minimize detection of ambient infrared light (e.g., IR light emitted by the laboratory's fluorescent lights or other hatching detectors). Silicone encapsulant (Q-Sil 216) was mixed and poured into the sleeves to pot the circuit boards and prevent corrosion when submerged in saltwater. The silicone was clear, with a refractive index of 1.406, which was comparable to that of 10 ºC, 35 ppt salinity seawater for 700 nm wavelength radiation, 1.337 (Austin & Halikas 1976). A vacuum chamber was used to degas the silicone after mixing and after pouring the silicone into the sleeves to ensure air bubbles did not obstruct the IR emitters or phototransistors and cause IR light to refract at an air/silicone interface. In spite of great care, some trapped air bubbles could not be removed, but the remaining sensors within the arrays provided adequate redundancy. An acrylic conformal coating was applied to the seal portions of the circuit board and electrical components that were not potted in silicone to provide corrosion resistance. These were the wireless transmitter, power and indicator LEDs, and the leads for the power supply.
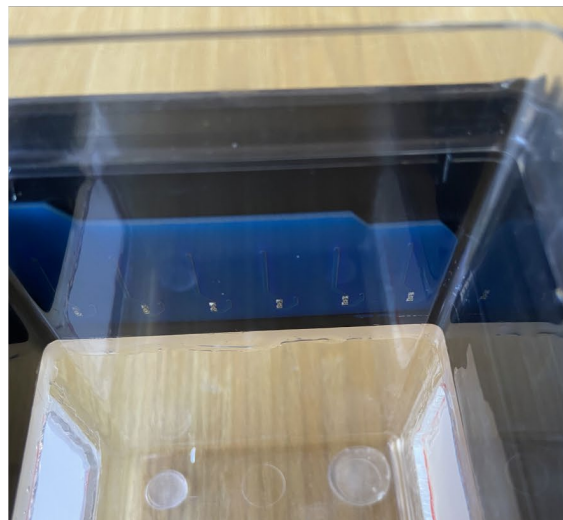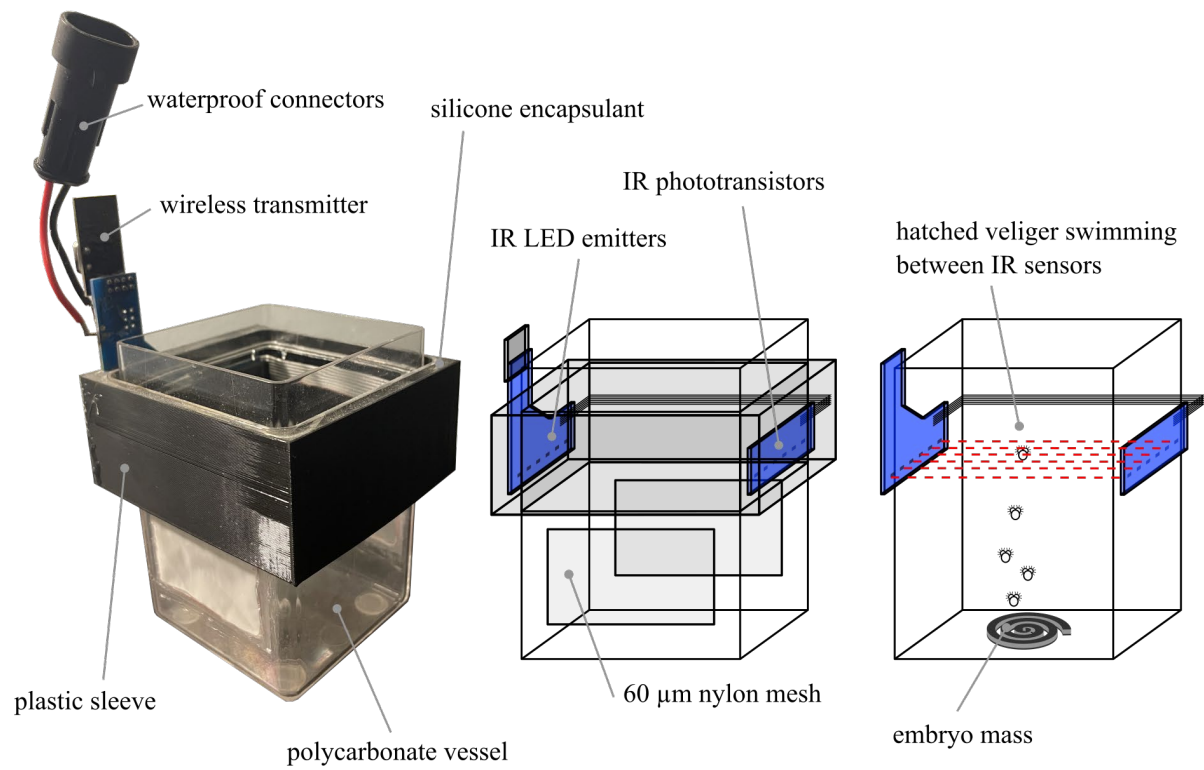
Figure 2.1. Photographs and schematics of hatching detectors with components labeled. The bottom photograph shows the IR phototransistor circuit board secured against the side of the vessel by the sleeve and waterproofed by clear silicone encapsulant.

Aquaria

Polycarbonate food pans (17.5 cm x 15.875 cm x 15.25 cm) were used as treatment aquaria to house the hatching detectors and the predator/non-predator chemical cue donor species (Figure 2.2). Short feet made of hot glue were added to the bottoms of the aquaria and hatching detectors to keep them level around uneven surfaces in the water table, to minimize sliding, and to allow water to flow underneath. Small sections of the pan lids were cut out to provide clearance for the wireless transmitters. ½-inch holes were drilled in opposite corners of the lids to support ½-inch PVC pipes to act as inlet and outlets for the water changing system. The inlet pipes measured 14 cm and the bottom edges were perforated with 1/16-inch holes and situated near the bottom of the aquaria. The outlet PVC pipes measured 8 cm and were situated so that the bottom edge was just above the water's surface. ½-inch plastic tubing was inserted into the lower ends to adapt to a 3/16-inch airline hose which could be attached to the automatic water change system. A short length of PVC pipe with insulation foam at the end was attached to the underside of the lid. When the lids were fastened to the aquaria with clips, the foam compressed and secured the hatching detectors in place to prevent organisms within the aquaria from repositioning or tipping over the hatching detectors. The aquaria were filled with 1.0 L of 0.45 µm vacuum filtered seawater collected from Shannon Point Marine Center in Anacortes, WA. Predator and non-predator cue specimens (e.g., crabs, shrimp, snails) were fed prior to being placed in the aquaria and swapped out with other fed individuals every 4 days during water changes. The mechanical cue (i.e., simulated predator attack) was applied by unplugging sensors, opening the lids, tearing the outer envelope of the embryo mass with forceps, reattaching the lids, and plugging sensors in 3 minutes later.

The hatching detectors were designed to be used in a water table (Figure 2.3). The water table that I used could accommodate 36 aquaria arranged in 3 rows and 12 columns. A water chiller set to 54 °F (11.66 °C) led into a manifold built from PVC and ball valves to distribute the chilled water evenly along the length of the water table to minimize temperature gradients. Three power supplies situated above the water table were used to power the hatching detectors. Waterproof connectors were used to attach the hatching detectors to the power supplies. To aerate the aquaria, two manifolds were constructed from 1/2-inch PVC tubing, each attached to several 4-way gang valves. Airline tubing was attached to the gang valves and the free ends with cylinder bubble stones were fed though the inlet PVC pipes of the aquaria. The gang valves were carefully tuned to sufficiently aerate the aquaria without generating too many bubbles and splashing that would risk shorting the electronics.

An automatic water change system was constructed to minimize the disturbance of egg masses and hatching detectors as well as facilitate water changing. Fifty percent water changes (0.5 L) were performed for all aquaria every four days. Normally, water changes are a two-step process: siphoning out water from the aquaria and then replacing it with 'clean' water. However, removing water from the aquaria causes two critical problems: the hatching detectors would gain enough buoyancy to tip in the water table and short the electronics, and the water level would dip below the sensor array, causing the IR sensors to max-out and disrupt data collection. A small shop vacuum was attached to one end of ½-inch PVC pipe with the opposite end capped. Three holes were drilled along the length of the PVC pipe and threaded to accept pipe-to-hose connectors which in turn could be attached to the outlets of three aquaria (i.e., each column of aquaria in the water table). Because the outlet pipes were situated just above the water's surface, the shop vacuum would only pull water out of the aquaria when the volume exceeded 1.0 L.

15

Funnels were placed in the aquaria inlet pipes so that recently filtered 'clean' water could be poured into one corner of the aquaria, causing 'dirty' water to get suctioned from the opposite corner. The process was repeated for all twelve columns.
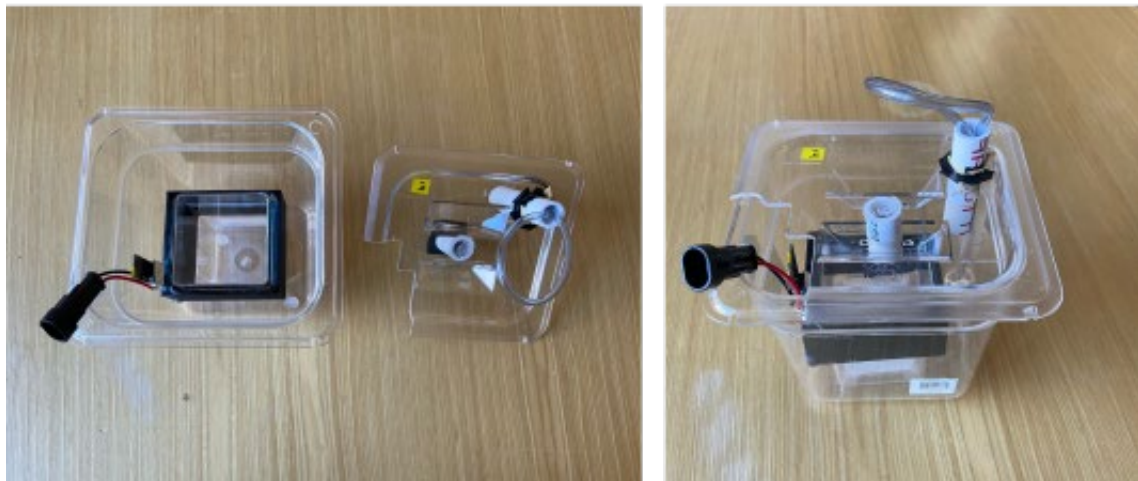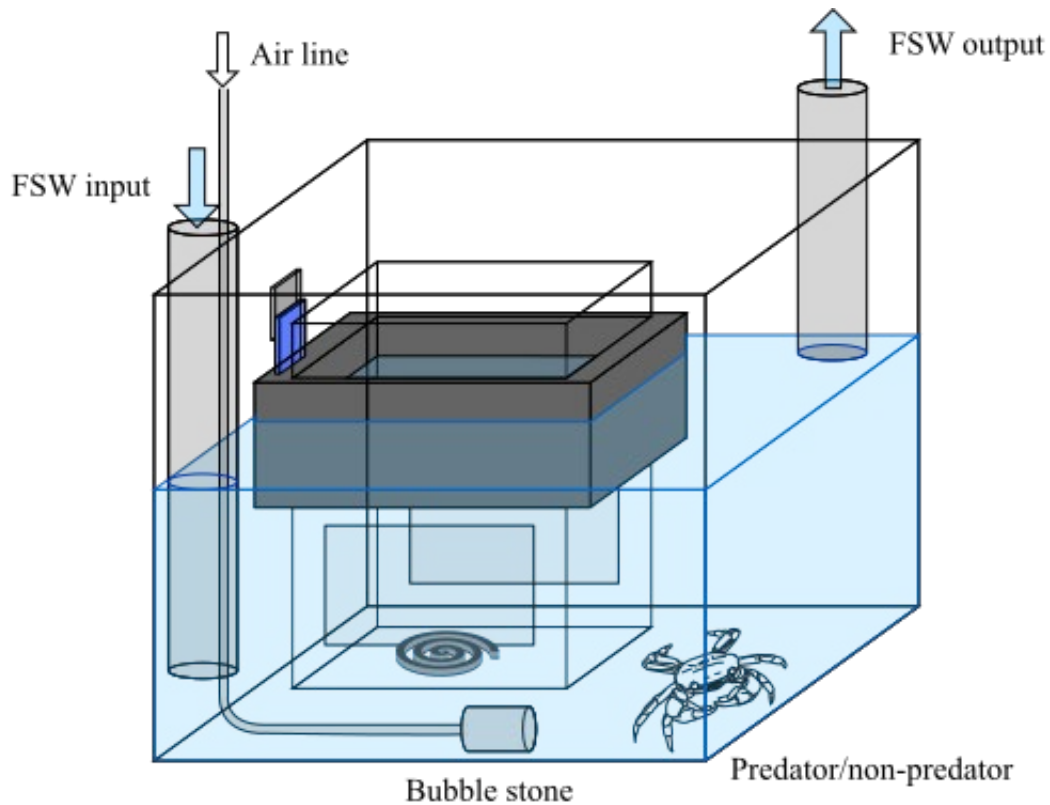
Figure 2.2. Diagram and photographs of treatment aquaria. Diagram incudes predator/non-predator specimen releasing kairomones, filtered seawater (FSW) in blue, and the arrangement of input and output PVC tubes for rapid water changes without affecting water depth. The photographs shows the aquaria and detector units (excluding the FSW input tube) assembled without the lid (left) and fully assembled (right).
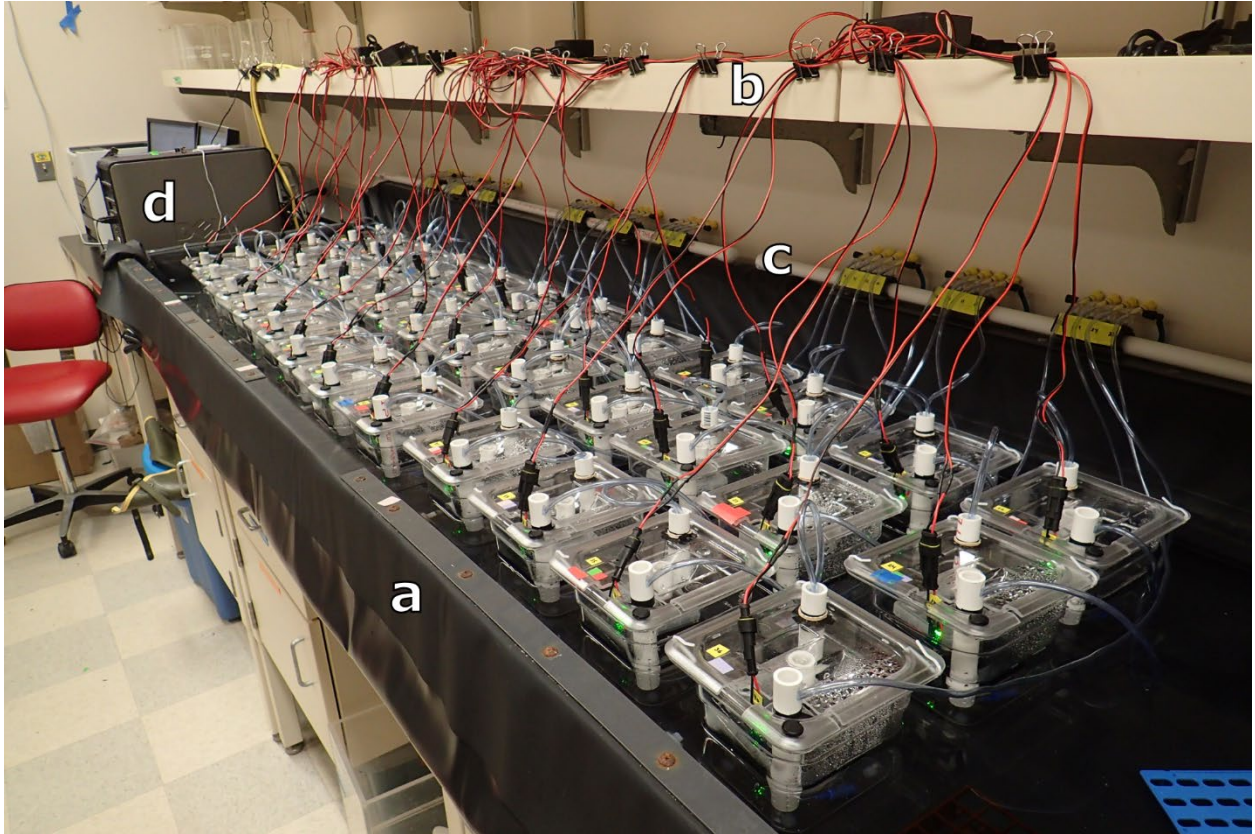
Figure 2.3. Experimental setup for *Hermissenda crassicornis* hatching plasticity experiment: **a**) water table with 36 treatment aquaria; **b**) power supplies and leads to each hatching detector; **c**) air supply manifolds with gang valves splitting airlines to each aquarium; **d**) Work station with wireless receiver to record transmissions from hatching detectors.

Data collection

I was able to monitor the hatching activity of egg masses in near real-time by processing the transmissions from the sensors and plotting the data in Rstudio. Each of the six emitter/phototransistor pairs from each hatching detector repeatedly sampled measurements of IR light intensity, concurrently calculating the exponentially weighted moving average and exponentially weighted moving variance. After each sensor collected 1,000 samples, roughly every five seconds, the hatching detectors sent these transmissions along with the hatching detectors' unique identification numbers. These transmissions were received by a workstation via a USB-to-serial adapter connected to a microcontroller with a wireless radio identical to the radios on the hatching detectors that was programmed to output all data received by the hatching detectors. All transmission were recorded and timestamped into separate lines within a comma separated text file using the CoolTerm freeware program. The data recordings were reset with a new file name every day to prevent file sizes from becoming too large, which would otherwise interfere with the program's ability to transcribe the transmissions with full fidelity.

R (R Core Team) was used to stitch the comma-separated text files together and plot the data from each hatching detector in quasi real-time (Figure 2.4, Appendix C). This allowed me to determine whether egg masses had begun hatching and helped determine if sensors stopped functioning properly. Several functions were written to plot data from all chambers or specific chambers, just the exponentially weighted mean or variance, and restrict the time ranges of the plots.

The exponentially weighted moving average values returned by the sensors were useful in determining whether sensors were functioning correctly (Figure 2.5, upper facets). Veliger larvae are mostly translucent and even in high densities after hatching, the exponentially

weighted moving average values wavered but did not decrease appreciably. If more than three of the six sensors of a hatching detector ceased to function (due to faults in fabrication or wear from use, such as shorting via corrosion) and hatching activity was not yet observed, the egg mass was carefully placed into another hatching detector and repairs were attempted for the faulty hatching detector.

The exponentially weighted moving variance values were much more useful for monitoring hatching activity and estimating hatch timing (Figure 2.5, lower facets). Upon setting up an aquarium and its hatching detector and powering it up, some level of variability was typical but generally settled to a background level after a few minutes. This background level was maintained in most cases until hatching, at which point the moving variance increased noticeably for most of the sensors. However, in spite of using filtered seawater and great care, some non-nudibranch species (e.g., ciliates or copepods) would occasionally swim in front of the IR sensors and add noise to the datasets. Although the specific timing of hatching for each sensor was determined after completing the in-lab experiments, hatching activity was generally characterized during experiments by a sustained period of high variability measured by multiple sensors, opposed to a short-lived increase in activity reported by a single sensor.
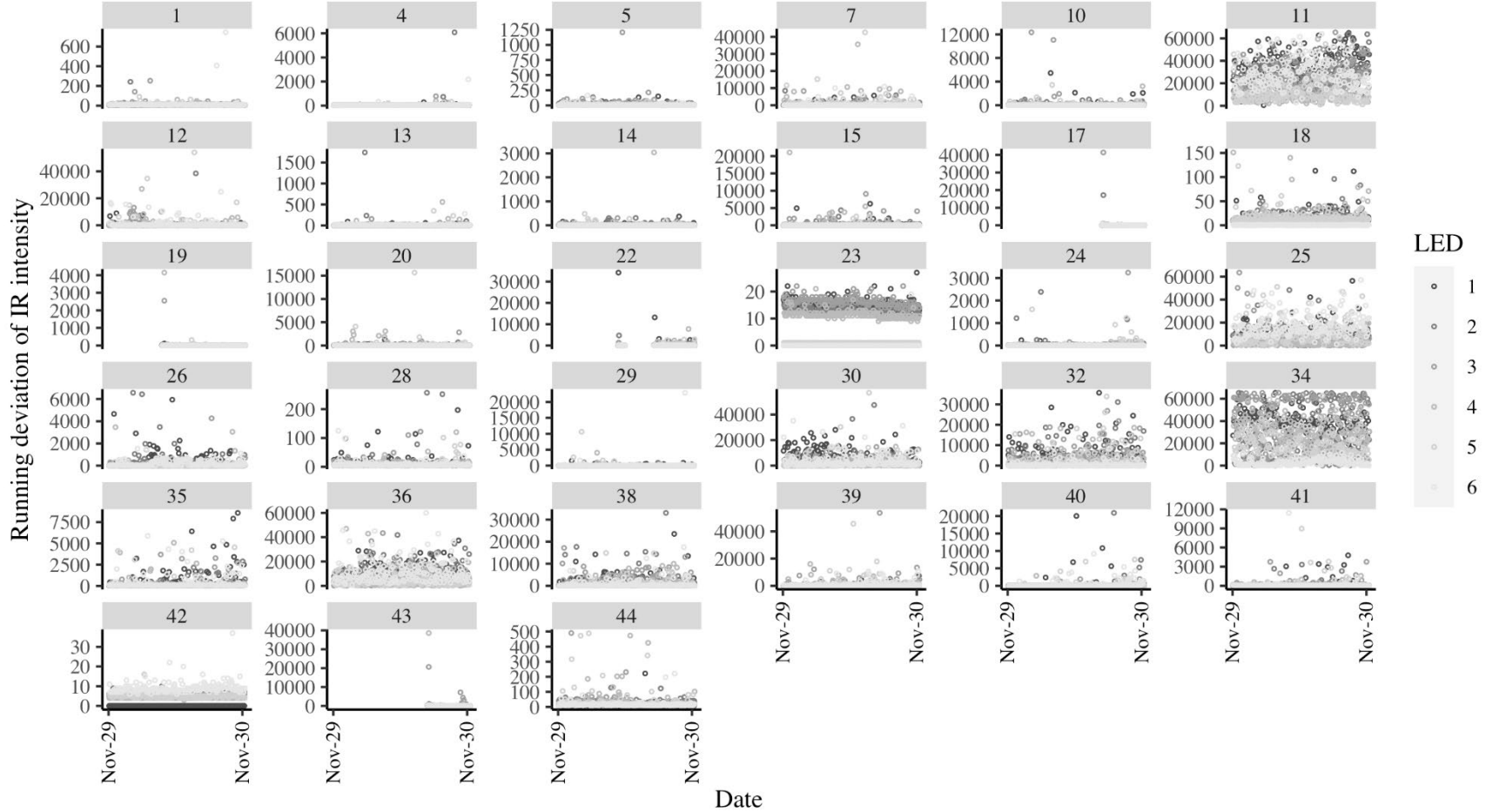
Figure 2.4. Sample dashboard for quasi real-time monitoring of hatching activity in *Hermissenda crassicornis* embryo masses. Each facet represents the most recent 24 hours of raw measurements of exponentially weighted moving variance of infrared light intensity from 6 independent infrared emitter/phototransistor pairs situated above a single embryo mass within a hatching detector. As veliger larvae hatch and swim across these sensors, the variance in the measured light intensity increases.
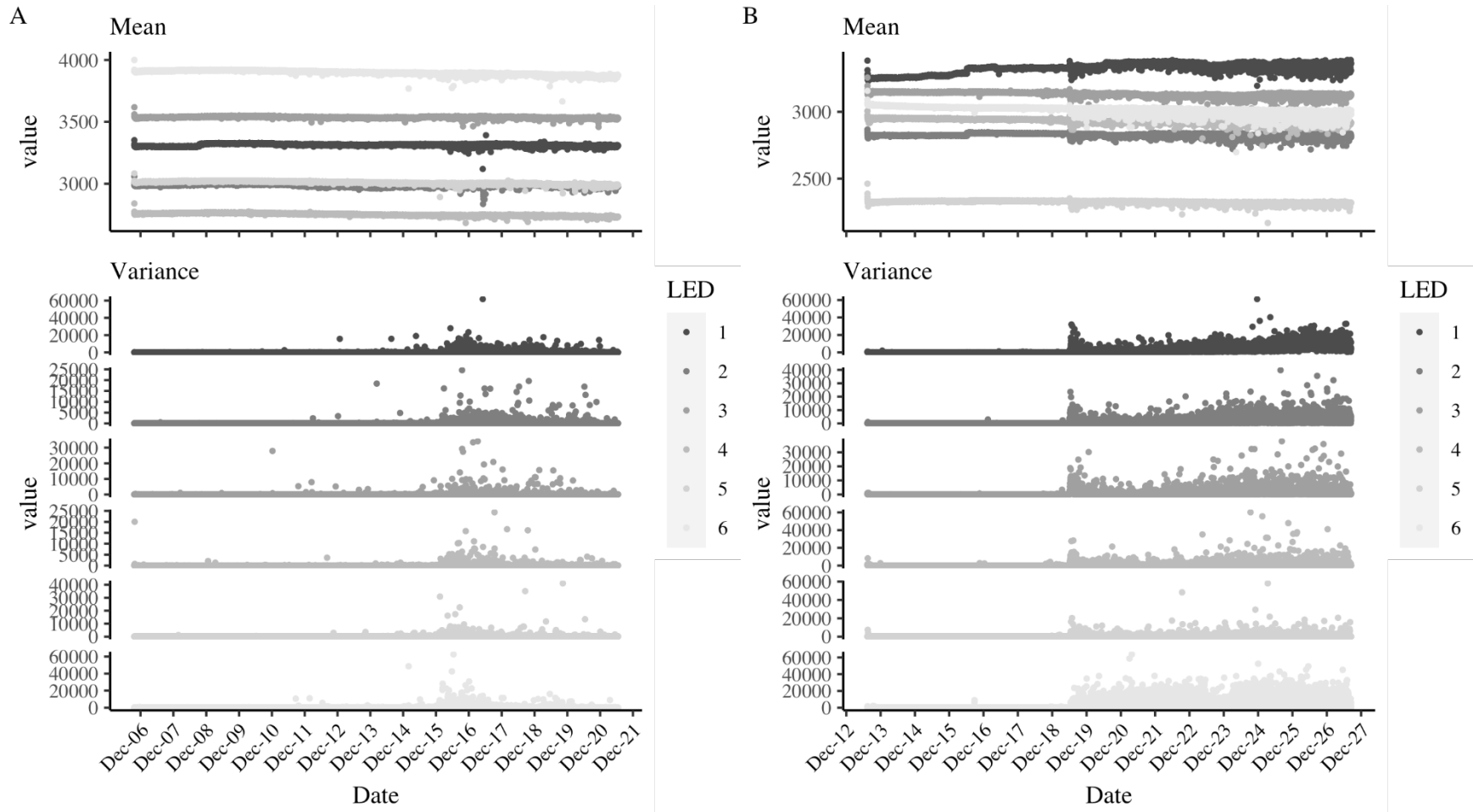
Figure 2.5. Example visualizations of raw sensor data from hatching activity of two *Hermissenda crassicornis* for embryo masses (**A**) one left undisturbed and (**B**) one with simulated predator attack seven days after oviposition. Each plot displays the raw exponentially weighted moving average (upper facet) and variance values (lower facet) from each of the 6 infrared emitter/phototransistor pairs (indicated by shading) within each hatching detector.

22

Hatch detection analysis

The timing of hatching of the egg masses was determined after completing hatching experiments in the laboratory. The raw hatching data for each egg mass were collated from the comma separated text files and exported into separate files for ease of use. Data collections typically continued for several days after hatching was first detected, so each time series spanned approximately 16 days. Each hatching detector sent transmissions every 4-5 seconds, resulting in six moving average and six moving variance estimates at approximately 300,000 discrete time points. Data from improperly functioning sensors within the arrays, characterized by mean or variance IR intensity readings that maintained constant values throughout the duration, were identified and excluded from the analysis.

The R script used to de-noise the raw datasets and identify hatch timing are provided in Appendix D. Some simplification was performed to reduce the computational demand and computing time (Figure 2.6, Figure 2.7). The first 12 hours of data collected by the sensors were trimmed off to exclude any disturbances caused from the initial setup of the aquaria. For each sensor of each detector, the 0.995 quantile was calculated and used to exclude outliers; such extreme values were much higher than those that typically indicate hatching. Then, the moving variance estimates for each functioning sensor were scaled to have a standard deviation of 1. For each 3-minute interval, the population standard deviation of the scaled moving variance values was calculated, which reduced the number of time points from ~300,000 to 7,000 for each sensor. The cumulative sum of these variance values was then calculated for each sensor, from which the area under the curve was estimated. The area under the curve estimates were used to again rescale the variance values so that each sensor's area under the curve was equivalent. This transformation made it possible to compare the variance values (i.e., hatching activity) of the

sensors at each time point and merge the signals from all sensors into one. Within each time point, the sensor with the maximum value was excluded to prevent a single high reading from indicating hatching activity and values from the remaining sensors were averaged. In other words, hatching is signaled when multiple sensors continuously detect increasing variance in IR intensity. A smoother using a rolling mean (window width of 15) was then applied, finalizing the simplified dataset.

The 'CE.Normal.MeanVar' function within the 'breakpoint' R package was used to determine the time-of-hatching (Priyadarshana & Sofronov 2016) from the simplified datasets. The function identifies the locations of breakpoints within a continuous dataset based on changes in both mean and variance. Although the function can be used to estimate the number of breakpoints, it was parameterized to search for only one breakpoint (i.e., time of hatching). Due to the sensitivity of this function, it was necessary to remove outliers and apply smoothers in the preparation of the simplified dataset. Additionally, because the CE.Normal.MeanVar function operates stochastically by iteratively sampling and refining possible breakpoints to maximize log likelihoods, reducing the dataset size was necessary to reduce computing times. The hatch times associated with the breakpoints were subtracted from the oviposition times to calculate time-to-hatching.

For each replicate (each with running mean and variance time series from 6 IR sensors)

Omit all measurements from any malfunctioning IR sensors

For running variance values of each functioning IR sensor:
  Trim first 12 hours
  Exclude outliers (> 0.995 quantile)
  Scale values to have standard deviation of 1
  Calculate standard deviation for each 3-minute interval
  ↳ **Reduced time series from ~300K to 7k points per sensor**

Calculate area under the curve (AUC) of cumulative sum for each sensor
Scale values for each sensor sensors using ratio of AUC / maximum AUC

For each 3-minute interval:
  Exclude sensor with highest value
  Calculate mean from remaining values
  ↳ **Single time series of hatching activity**

Calculate rolling mean with window width of 15
  ↳ **Final time series**

CE.Normal.MeanVar from *breakpoint* package in *R*
  ↳ **Identify location of single breakpoint**

Time-to-hatching = hatch time - oviposition time

Figure 2.6. De-noising and hatch timing analysis procedure. The raw data from the hatching detectors required de-noising, rescaling, and summarizing prior to the breakpoint analysis that ultimately determined when hatching occurred. These steps were necessary to omit outliers, reduce the number of points in the time series, and prevent any one sensor from dominating the signal.
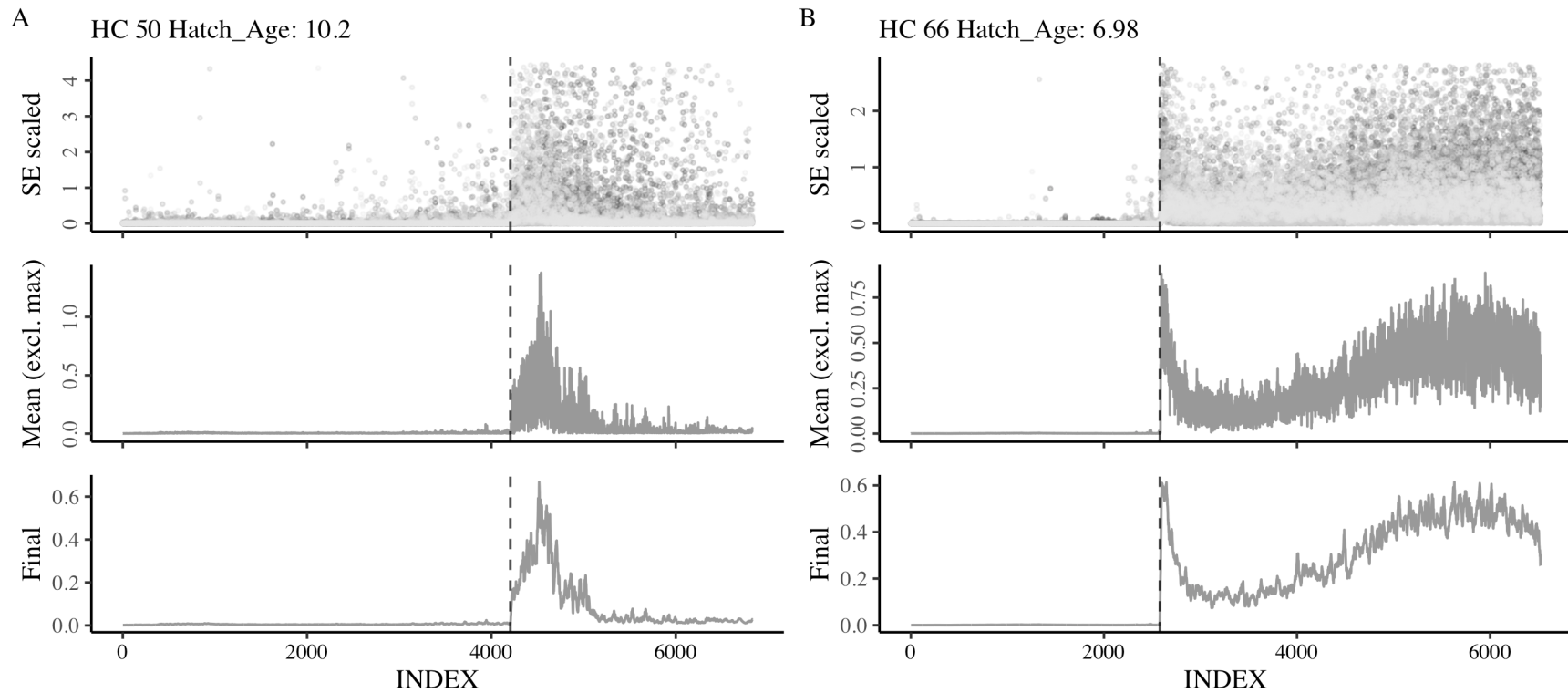
Figure 2.7. Example visualizations of de-noising and hatch timing determination from two *Hermissenda crassicornis* embryo masses,

(**A**) one left undisturbed and (**B**) one with simulated predator attack seven days after oviposition. The x-axis represents time, where

each x-value is a summary of exponentially weighted moving variance of infrared light intensity from 6 independent

emitter/phototransistor pairs within a 3-minute interval. Each plot shows (upper facet) de-noised and rescaled measurements of,

(middle facet) average of the previous values at each time point excluding the sensor with the maximum value, and (lower facet) the

finalized time series used for the breakpoint analysis, which results from calculating the moving average of the previous values as a

final smoother. The black dashed line indicates the breakpoint identified by the breakpoint analysis

26

Future design considerations

Generally, the hatching detectors performed well and their utility in determining hatch timing within PIHP experiments is demonstrated in Chapter 3. However, I suggest improvements to both the design of the sensors and how they are used that might improve their performance and increase their utility.

Forty-three hatching detectors were constructed, 40 of which had at least four of six IR sensors functioning nominally, where mean measurements were below the maximum value of 4,092 and variance measurements responded to disturbances. The three remaining hatching detectors had 3 functioning sensors, so these were employed in hatching tests when no other detectors were available. However, at the end of both hatching experiments, six of the sensors sustained corrosion damage and ceased transmissions. In spite of adding several applications of acrylic conformal coating to protect the portions of the boards that were not potted in silicone, the bubble stones used for aeration likely created enough water vapor to cause corrosion, usually around the power supply leads. Between uses, epoxy was applied to where the power supply leads met the boards to reinforce the corrosion protection, which usually prevented further problems. The boards were designed with the power supply leads, LEDS, and Bluetooth transmitter excluded from the silicone, so future designs should at the minimum consider potting the power supply leads.

The hatching detectors were not calibrated to provide estimates of larval concentration. The hatching detectors could have been tested with known concentrations of veliger larvae which should allow experimenters to not only quantify the time of first hatching but also potentially quantify hatching rates. In such an application, cetyl alcohol flakes should be used to

reduce the surface tension so that hatched larvae do not accumulate at the water's surface above the sensors (Hurst 1967).

On a few occasions, hatching activity was so rapid and intense that the exponentially weighted moving variance values calculated by the hatching detectors exceeded the maximum value that could be stored by the number of bits (65,535). In such cases, these large values were bit-shifted such that a value such as 70,000 was returned as $70,000 - 65,535 = 4,465$. This issue did not seem to have an influence on the time-to-hatching analysis, but future iterations of the IR transmitter board script should consider allocating more bits to the moving variance values calculated by the sensors.

Many embryo masses failed to hatch in the hatching experiments. Within the hatching experiments for *H. crassicornis*, 17 of 67 embryo masses did not hatch, and 3 of 19 failed to hatch within the *O. bilamellata* hatching experiments. Before being placed into the hatching detectors, the embryo masses were confirmed to be fertilized (e.g., past the 1-cell stage) using a dissecting microscope. During the breakdown of the sensors, the developing embryos were found at varying stages of development which implies conditions were suboptimal for either development or survival. FSW was used as a precaution to minimize concentrations of parasites and other organisms from interfering with the measurements of the hatching detectors or consuming unhatched embryo. In spite of using FSW, inspections of the hatching detectors after hatching often found microorganisms that were either not properly filtered or were stowaways on the individuals added to the aquaria to provide chemical cues. It is possible that these microorganisms played a role in degrading embryo masses and actually facilitating hatching (Harris 1975). Harris suggested in his observations of several nudibranch species that the other organisms inhabiting the embryo mass did not attack the developing veligers and that this

phenomenon might be common among nudibranchs. Future work is needed to determine if using FSW with the hatching detectors is unnecessary, in addition to considering the cost of filters and time required to vacuum-filter seawater.

The toxicity of materials used in the construction of the sensors and inadequate aeration might have also contributed to hatching failure. The effect of the toxicity of the materials used to construct the sensors is unknown but great care was taken to waterproof all electrical components to prevent leaching of residues of materials such as lead solder, flux, and isopropyl alcohol in addition to preventing corrosion. After construction and before and after uses, the hatching detectors were rinsed with deionized water to minimize contamination and corrosion.

The extent of aeration provided by the bubble stones was likely variable between containers because the manifold and gang valve systems were adjusted by eye until all bubble stones were visibly releasing air but not violently bubbling. Although dissolved oxygen concentration was not measured during the experiments, the importance of adequate aeration for proper development is well-documented (Hurst 1967, Strathmann & Chaffee 1984) and the gel of embryo masses acts as the main inhibitor of oxygen transport (Moran & Woods 2007). It is also possible that burrowing nematodes and other microorganisms that mechanically break down embryo masses also promote aeration, but these were filtered out.

Conclusions

The hatching detectors measured changes in hatching activity and the data were interpreted to generate reasonable estimates of hatch timing with high temporal resolution (3-min intervals). The hatching detector design accommodated the testing of both mechanical and chemical cue factors. The chemical cue donors suffered no mortalities while in the hatching

detectors. The mesh of the hatching detectors separated chemical cue donors from the embryo mass and hatched veligers while allowing the diffusion of oxygen and chemical cues. The simulated predator attacks typically did not disrupt data collection and cases where variance values did seem to be affected were easily differentiated from hatching activity as short, unstained deviances from background signals. Although there are several improvements that could be made in the sensor design and program scripts to improve their durability and utility, the designs presented here represent a novel use of IR light to detect hatching and quantify hatch timing. The hatching detectors were employed on nudibranch species but should be applicable to any organism with near-microscopic swimming larvae that hatch from benthic embryo masses.

Chapter 3: Hatching Plasticity Experiments

Introduction

Many species have complex life-histories and when individuals undergo ontogenetic niche-shifts is an important plastic response with cascading effects on how they interact with environment and its cohabitants. For many fish species, changes in resource use and predation risk are continuous with growth, and the size and type of both prey and predators scale with body size. In species that metamorphose, like amphibians and insects, niche-shifts are more abrupt as wholly different habitats are utilized with different resources and predators (Werner & Gilliam 1984). Whether an organism is hatching, reaching metamorphosis, or at the onset of reproduction, they must not only make an appropriate response of what to do in preparation for the switch point, but must also pick the appropriate time to do it (Sih & Moore 1993, Chivers 2001, Agrawal 2001). Failure to choose the optimal timing of niche switching results in increased threat of predation, lost opportunity to feed or mate, or higher competition for limited resources.

Hatching is perhaps the earliest ontogenetic niche-shift and its timing exerts high leverage on an organism's fitness (Warkentin 2007). Many organisms, including amphibians, reptiles, birds, and invertebrates encapsulate their offspring in aggregate masses where they develop before hatching (Pechenik 1979, Sih & Moore 1993, Warkentin 2011). With limited mobility, embryos are highly susceptible to extreme abiotic conditions (Armstrong et al. 2013) or predation (Chivers et al. 2001, Orians & Jensen 1974, Warkentin 2001, Vonesh 2005, Vonesh & Bolker 2005) and rely on either their own limited sensory capabilities, or in some instances, their parents (Li 2002), to choose the optimal time to hatch to avoid unfavorable conditions before and after hatching. Predator-induced hatching plasticity (PIHP) in particular is interesting because of

underestimating predation threat either before and after hatching can have immediately dire consequences.

The most well-studied cases of PIHP are with amphibians. Salamanders that detected chemical cues from predatory flatworms delayed hatching in order to hatch at a larger size. Smaller newly-hatched larvae are more susceptible to predation (Sih & Moore 1993), and in this example, the post-hatching life stage is deemed higher-risk than the incubation stage, and delaying hatching results in improved survival. However, arboreal egg clutches of a tree frog species hatch early in response to attacks from snakes and escape predation by falling into ponds below. Although smaller tadpoles are more vulnerable to aquatic predators and their ability to feed is delayed, immediately making a niche-shift from the high-risk arboreal habitat to an aquatic habitat of unknown risk improves survival (Warkentin 1995).

An adaptive trait such as the ability to modify hatch timing benefits individuals when the level of predatory threat is correctly detected, and the response to accelerate or delay hatching depends on which life stage is threatened. A poor assessment of risk and an incorrect response results in lower fitness (Ydenberg & Dill 1986). Naturally, underestimating the predatory threat results in a higher likelihood of being consumed. Similarly, individuals that overestimate the predatory threat might unnecessarily delay their development at later life stages, make themselves more vulnerable to predation in the next life stage by hatching prematurely, or face higher interspecific and intraspecific competition to acquire resources (e.g., food, real estate) by unnecessarily delaying hatching.

Prey species, including unhatched embryos, have several ways of assessing their threat of being consumed by predators. Prey species might detect kairomones, or chemical cues, of their predator (Dodson 1989), such as in the previously mentioned case of salamanders delaying

hatching when flatworms kairomones are detected in the water (Sih & Moore 1993). Such cues are proximate measures of predation threat. A higher concentration of kairomones may imply an increased predation threat and higher confidence in the risk assessment; it by no means guarantee that predation will occur, but can provide enough forewarning to invest in a response, such as modifying development rates (Warkentin 2011).

Mechanical stimuli provide shorter notice for predation than chemical cues but can be interpreted as a higher predation threat with higher confidence, such as with the previously mentioned tree frogs that hatch as an escape response to vibrational cues during attacks from snakes (Warkentin 1995, Warkentin 2005). Like chemical cues, mechanical stimuli from predators and non-predators can be distinguished from one another to prevent inappropriate predator escape or avoidance responses such as hatching in response to vibrations due to storms (Warkentin 2005). Unlike chemical cues, mechanical stimuli indicate an immediate threat and therefore any predator-induced hatch response is encouraged to be accelerated rather than delayed.

PIHP in the Marine Environment

Nearly all studies on predator-induced hatching plasticity have focused on terrestrial vertebrates (Warkentin 2007, Vonesh 2005) and arthropods (Li 2002, De Roeck et al. 2005) but PIHP in marine invertebrates is likely more common than represented in the literature, given the similarities in embryonic/larval life histories. At least four phyla of marine invertebrates (Annelida, Mollusca, Nemertea, and Platyhelminthes) oviposit embryos in benthic aggregations (Pechenik 1986, Harmon & Allen 2018), and such demersal eggs have particularly high predation pressure (Orians and Janzen 1974). Offspring go through several life history switch

points as they transition between habitats during larval, juvenile, and adult stages. Miner et al. (2010) documented the first case of predator-induced hatchling plasticity within Lophotrochozoa, in a nucellid snail. Benthic juveniles delayed hatching from egg capsules in response to chemical cues from crab predators. Additionally, Strathmann et al. (2010) documented accelerated time-to-hatching in the tropical nudibranch *Phestilla sibogae* by simulating predatory attacks through mechanical disruption of the gelatinous envelopes of embryo masses. To my knowledge, no PIHP studies have been performed on any other nudibranch species. Further investigation of this phenomenon in marine invertebrates is needed to determine if predator-induced hatching plasticity is common within the Lophotrochozoa, but also to the diverse taxa that exhibit similar life histories and reproductive strategies.

To date, no studies have utilized a fully factorial study design to investigate PIHP in response to both mechanical and chemical cues in a marine species. Additionally, only two PIHP studies have considered physical and chemical cues simultaneously, both with frog species; one without a factorial design (Smith & Fortune 2009) and one with a factorial design to evaluate additive and interactive effects (Poo & Bickford 2014). This is surprising given how these cues might indicate different levels of predation risk. For instance, chronic chemical cues may not necessarily be reliably interpreted as imminent predation risk, but development times may be modified so that hatching occurs in a way that avoids predators. By contrast, an acute physical cue such as tearing of the embryo mass or violent vibration might be reliably interpreted as an imminent threat and induce hatching. Coupled together, an embryo that developed quicker in response to chemical cues from a predator may also gain competences earlier to sense physical cues from a predator and also hatch in an effort to escape an attack. The hatching detectors described in the previous chapter were designed specifically so that hatch timing of benthic

35

embryo masses could be quantified in an experimental design with a chemical cue factor and a physical cue factor fully crossed.

Study overview

Using specifically designed hatching detectors, I investigated whether two nudibranch species, *Hermissenda crassicornis* and *Onchidoris bilamellata*, modify hatch timing in response to predators. I first performed simple feeding tests of embryo masses using a variety of more common benthic intertidal fauna to identify potential predators for hatching plasticity experiments. After identifying likely predators and non-predators of the embryo masses, I exposed the embryo masses to chemical cues from those species to represent a chronic predation risk. Additionally, in the *H. crassicornis* hatching plasticity experiment, I employed a fully factorial design to cross the chemical cue with an acute mechanical cue – a simulated attack from a predator via tearing of the outer envelope of the embryo mass – to determine whether hatch timing is affected by the cues independently or via an interaction. Following the reasoning that hatching prematurely allows planktonic larvae to escape from benthic predators, I predicted that larvae from both species would hatch sooner in response to both chemical cues from predators (versus non-predators and no chemical cue) and mechanical disruption (versus no simulated attack), and I also hypothesized that these two cues will induce a faster time-to-hatching together than individually.

Methods

Study Organisms

Hermissenda crassicornis and *O. bilamellata* area ideal candidates as two temperate

nudibranch species in which to investigate PIHP. Both species go through indirect development

with feeding and swimming planktotrophic veliger stages that exhibit negative geotaxis;

therefore, these species are ideal for performing hatching plasticity studies with the

aforementioned hatching detectors. The methods for rearing *H. crassicornis* and *O. bilamellata*

in the laboratory are well-documented (Harrigan & Alkon 1978, Williams 1980, Chia and Koss

1988, Avila et al. 1998). In the Salish Sea, adult *H. crassicornis* are easily collected from the

intertidal during low tides or from dock pilings, produce embryo masses year-round, and are

easily cared for in the laboratory. *O. bilamellata* are also easily collected from pilings and under

rocks in during moderately low tides, but are seasonally abundant in the northeast Pacific,

typically during December and January during spawning (Hurst 1967, Bleakney & Saunders

1978, Todd & Doyle 1981).

Hermissenda crassicornis is an aeolid nudibranch that is common in the intertidal and

subtidal zones from Alaska to Northern California (Lindsay & Valdés 2016) and is an important

model organism for studies in memory, learning, and behavior (Alkon 1983). It is known to

thrive in different habitats (Gotshall and Laurent 1980), and feeds on a variety of species such as

hydroids, tunicates, and anemones (Megina et al. 2007). As simultaneous hermaphrodites, these

nudibranchs perform reciprocal fertilization and produce benthic embryo masses on average 2.64

days (sd = 1.33 days, n = 20) after copulation (Rutowski 1983), each with 7,000 to one million

embryos (Avila et al. 1997). The literature regarding the incubation period before the

planktotrophic veligers hatch suggests this process is temperature dependent: 5-6 days after

incubation and teasing of the embryo mass at 13-15 ºC (Harrigan & Alkon 1978), or after 7 days

at 14 ºC (Williams 1980). The planktrophic veliger larvae are approximately 102 μm across at

hatching (Hurst 1967, Williams 1980) and metamorphose into juveniles after 34-58 days

(Harrigan and Alkon 1978).

Onchidoris bilamellata is a common dorid nudibranch on the temperate and subarctic

intertidal rocky shores of the northern hemisphere, ranging from Alaska to California and Japan

in the Pacific Ocean and the Atlantic coasts of Connecticut to Greenland, and England (Bleakney

& Saunders 1978). It is a voracious predator of barnacles, particularly Balanus balanoides (Todd

& Doyle 1981), whose chemical cues induce settling and metamorphic competence (Chia and

Koss 1988). Adults typically die off after spawning, which occurs approximately 3-months after

first settling (Todd 1981). O. bilamellata have discrete breeding seasons and no overlap between

generations and therefore might rely on adaptations (Todd and Doyle 1981), such as hatching

plasticity in response to embryo predation to prevent reproductive failure. The embryonic period

lasts approximately 12-13 days at 11 ºC (Hurst 1967) or as long as 5.5 weeks at 4-6 ºC (Barbeau

2004). The hatched veligers are approximately 150 μm across (Hurst 1967) and reach

metamorphic competence after 28-32 days at 11 ºC or 60-80 days at 7.5 ºC (Chia & Koss 1988,

Barbeau et al. 2004).

The literature regarding what consumes northeast Pacific nudibranch embryo masses is

scant, but the sacoglossan Olea hansineensis has be documented to consume embryo masses of

H. crassicornis in addition to those of two other nudibranch species, Dendronotus iris and

Archidoris montereynsis, in a laboratory setting (Crane 1971). O. hansineensis consumes

embryos by slipping head first into the embryo mass and using a muscular pharynx to pump

embryos into its mouth. However, the distribution of O. hansineensis is not as widespread as that

of *H. crassicornis* or *O. bilamellata* and is apparently restricted to select *Zostera marina* eelgrass beds in Friday Harbor, WA, Tofino, BC, and Tuwanek, BC (Crane 1971, Millen 1980). Although *O. hansineensis* seems to be the only documented predator of *H. crassicornis* embryo masses, its small size of 1-7 mm (Crane 1971), manner of feeding that is difficult to simulate, and limited distribution made it logistically complicated to collect and include in the following PIHP experiment. I was unable to find any literature on what predates upon *O. bilamellata* embryo masses, but juveniles and adults of the species are known to produce a mucus to make themselves unpalatable to predators (Potts 1981). Whether adult *H. crassicornis* or *O. bilamellata* confer chemical defenses to their offspring or their embryo masses is unknown, but one tropical nudibranch species, *Hexabranchus sanguineus*, passes chemical compounds derived from the sponges they consume to their embryo masses for antimicrobial and presumably, antipredator defence (Pawlick et al. 1988). A small palatability study in the San Juan Islands observed no predation of on the embryo masses of the dorid nudibranch embryo masses from *Doris montereyensis* or *Diaulula sandiegensis* when presented to the crab species *Chionoecetes bairdi*, *Oregonia gracilis*, and *Scyra acutifrons* (Chang 2014).

Theoretically, if *H. crassicornis* and/or *O. bilamellata* veligers hatch prematurely in response to chemical cues from predators, selective pressures would favor that the response would be specific to predators to avoid the costs of responding incorrectly to cues from a non-predator (Touchon et al. 2013). I performed simple feeding experiments to identify species that do or do not consume embryo masses with the purpose of identifying species to include as chemical cue donors in the hatching timing experiments; one to release predator chemical cues and another to release non-predator chemical cues, (alongside a control, no-cue level).

39

Specimen collection and maintenance

I maintained all collected specimens in aquaria within an 11 °C cold room at Western Washington University, each filled with unfiltered seawater from the Shannon Point Marine Center in Anacortes, WA. Every four days, I changed 50% of the water volume and removed any rotting material. Experiments were performed in a nearby ambient-temperature laboratory equipped with a water table circulating 12 °C refrigerated freshwater.

I collected *H. crassicornis* and *O. bilamellata* from the docks at the Anacortes Marina and housed them in 10-gal aquaria. I fed the *H. crassicornis* the thecate hydroid *Obelia dichotoma* that were collected from the same docks as well as shelled *Mytlius edulis* collected from the Port of Bellingham Bay Marine Park. *O. bilamellata* were fed barnacles on encrusted rocks collected from Port of Bellingham Bay Marine Park. *H. crassicornis* and *O. bilamellata* oviposited embryo masses on their food as well as on the sides of the aquarium. I collected embryo masses over a 3-day period and maintained them in aerated containers until the day of the feeding test.

Several candidate predator and non-predator species were collected from the docks at Anacortes Marina, and the rocky intertidal at Shannon Point Marine Center (list of species in Tables 3.1 and 3.2). I was able to collect both *Pugettia producta* and *Pugettia gracilis* from both locations, but the specimens in my preferred size range were more abundant in the rocky intertidal. I also collected the crab species *Glebocarcinus oregonensis, Petrolisthes eriomerus*, *Hemigrapsus nudus*, *Hemigrapsus oregonensis*, and *Lophopanopeus bellus* from Shannon Pont, the shrimp species *Heptacarpus brevirostris* from the same docks as the nudibranchs at Anacortes Marina, and the snail *Nucella lamellosa* from the rocky low intertidal of Port of

Bellingham Bay Marine Park. I starved these specimens for 2 days prior to the embryo mass

predation experiment to promote active feeding.

Embryo mass vulnerability experiments

      I designed the following experiment to determine which species consume embryo masses

of *H. crassicornis* or *O. bilamellata.* The results of these experiments informed which species I

used to represent both predator and non-predator levels of the chemical cue factor in the hatching

plasticity experiments. Including both a non-predator chemical cue level alongside an

experimental control level was important because some plastic responses might be non-specific

and induced by both predator and non-predator species (Bourdeau & Padilla 2019). I placed

crystallizing dishes filled with raw seawater in the water table. Within each dish, I placed a

single *H. crassicornis* or *O. bilamellata* embryo mass and one specimen of a potential predator

species. Only recently oviposited embryo masses were used in these predation tests to minimize

the possibility that the embryo masses biofoul/decompose and give the appearance they were

handled by a predator. Over the course of three days, I made observations several times per day

and categorized these observations in increasingly convincing order of evidence of predation:

embryo mass intact and no signs of handling by the specimen; specimen directly observed

handling embryo mass but not actively tearing or consuming it; embryo mass was found

shredded or fragmented and assumed to be caused by the specimen; or specimen was witnessed

actively consuming the embryo masses. When possible, I collected video footage of the

specimens consuming the embryo masses.

Hermissenda crassicornis vulnerability experiment

Several species were identified as predators of *H. crassicornis* embryo masses (Table 3.1, Figure 3.1). I witnessed four of the five *Heptacarpus brevirostris* individuals actively feeding on the embryo masses, and although I did not observe the fifth individual consuming its embryo mass, I found the embryo mass in several pieces. Additionally, I witnessed both individuals of *Lophopanopeus bellus* tearing and consuming *H. crassicornis* embryo masses. *L. bellus* is an omnivore of algae, crustaceans, and mollusks (Knudsen 1964), so I considered its appetite for *H. crassicornis* embryo masses when starved as typical. I categorized both *H. brevirostris* and *L. bellus* as likely predators of *H. crassicornis* embryo masses. One of three *P. gracilis* individuals consumed the embryo mass, but I found no evidence of predation by the other two individuals. I considered *P. gracilis* a predator of *H. crassicornis* embryos but with a lesser voracity than that of *H. brevirostris* and *L. bellus*. I observed one of two *H. nudus* gently handling an embryo mass, but I did not see it tearing it apart or eating it. *H. nudus* is generally an herbivore of algae but may very occasionally consume meat as a predator or scavenger (Knudsen 1964), so I did not conclusively categorize *H. nudus* as a predator or non-predator of *H. crassicornis* embryo masses.

Four of the species surveyed in the embryo mass predation experiments did not give any indication that they consume *H. crassicornis* embryo masses: *P. eriomerus*, *G. oregonensis*, *P. producta*, and *H. oregonensis*. *Glebocarcinus oregonensis* is known to feed primarily on barnacles and secondarily on snails, bivalves, and worms, so it was somewhat surprising that they did not show interest in *H. crassicornis* embryo masses, even when starved. Both *H. oregonensis* and *P. product*a are known to feed primarily on kelp and algae and secondarily on animals such as barnacles and mussels if given the opportunity (Knudsen 1964), so it was also

surprising that they did not consume *H. crassicornis* embryos even when starved. *P. eriomerus* predominantly filter feeds on diatoms and is generally considered an herbivore (Knudsen 1964), so I was not surprised by their lack of interest in the nudibranch embryo masses. I categorized all four of these species as unlikely predators of *H. crassicornis* embryo masses.

Given the results of these predation experiments, I decided to use *H. brevirostris* as the predator level and *P. eriomerus* as the non-predator level of the chemical cue factor within the hatching plasticity experiments. Among the species categorized as non-predators of *H. crassicornis* embryo masses, I selected *P. eriomerus* as best non-predator candidate for the hatching plasticity experiments due to its strict reliance on filter feeding. Unlike the other crab and shrimp species surveyed, the chemical cues released by *P. eriomerus* should presumably not include those of consumed mollusk species. Although *L. bellus* also showed interested in *H. crassicornis* embryo masses, *H. brevirostris* were more abundant, easier to collect, and found in the same location as the *H. crassicornis*. Additionally, the shrimp *H. brevirostris* is more distantly-related to the anomuran crab *P. eriomerus* that I elected as the non-predator chemical cue, compared to the xanthid crab *L. bellus*.

Table 3.1. Results of the *Hermissenda crassicornis* embryo mass vulnerability experiment. All potential predator specimens were starved for 2 days prior to being isolated with a single *H. crassicornis* embryo mass and periodically observed over 3-4 days. Evidence of oophagy was categorized into three increasing levels: Individuals that were observed to handle embryo masses but not consume them provided the weakest evidence of oophagy; embryo masses that were found damaged but were not directly observed to be eaten; and direct observations of handling and consumption of embryo masses.

Family	Species	Witnessed handling	Found damaged	Witnessed consuming	Total
Porcellanidae	*Petrolisthes eriomerus*	0	0	0	0 of 2
Cancridae	*Glebocarcinus oregonensis*	0	0	0	0 of 2
Epialtidae	*Pugettia gracilis*	0	0	1	1 of 3
Epialtidae	*Pugettia producta*	0	0	0	0 of 2
Grapsidae	*Hemigrapsus oregonensis*	0	0	0	0 of 2
Grapsidae	*Hemigrapsus nudus*	1	0	0	1 of 2
Xanthidae	*Lophopanopeus bellus*	0	0	2	2 of 2
Hippolytidae	*Heptacarpus brevirostris*	0	1	4	5 of 5

Figure 3.1. Stills taken from video documenting ovipredation of nudibranch embryo masses. *Hermissenda crassicornis* embryo masses being consumed by (**upper left**) *Heptacarpus brevirostris*, (**bottom left**) *Pugettia gracilis*, and (**bottom right**) *Lophopanopeus bellus*. *Onchidoris bilamellata* embryo mass being consumed by (**upper right**) *Pugettia gracilis*, but this photo was taken separately from the vulnerability experiment.

Onchidoris bilamellata vulnerability experiment

As with the *H. crassicornis* embryo mass predation tests, *H. brevirostris* was observed as a predator of *O. bilamellata* embryo masses (Table 3.2). One specimen was witnessed consuming an embryo mass and all embryo masses in the three remaining replicates were found damaged. embryo masses in three of four replicates with *P. producta* were found damaged, and with both *P. gracilis* and *P. eriomerus,* two of four replicates each were found damaged. Given that *P. eriomerus* is a filter feeder, this result was surprising. It is possible that *P. eriomerus* did handle the embryo masses but unfortunately no handling or consumption was directly observed. The damage could also have been unintentional. It was also interesting that *P. producta* might consume *O. bilamellata* embryo masses when there was no apparent interest during the *H. crassicornis* embryo mass predation experiment. A single replicate of an *O. bilamellata* embryo mass with *H. oregonensis* was also found damaged. H. *oregonensis* generally feeds on algae and diatoms, but it known to opportunistically consume animals. *H. brevirostris* was the most aggressive predator of *O. bilamellata* embryo masses among the assayed species and was chosen to represent the predator level of the chemical cue factor in the hatching plasticity experiment.

Two of the seven species surveyed in the embryo mass predation experiments, *H. nudus* or *N. lamellosa*, did not present any indication that they consume *O. bilamellata* embryo masses. I elected to have the snail *N. lamellosa* represent the non-predator level of the chemical cue factor of the *O. bilamellata* hatching timing experiments because of the assumption that its chemical cues would be more different to those of the predator level, the shrimp *H. brevirostris*, compared to another crustacean such as *H. nudus*.

Table 3.2. Results of *Onchidoris bilamellata* embryo mass vulnerability experiment. All potential predator specimens were starved for 2 days prior to being isolated with a single *O. bilamellata* embryo mass and periodically observed over 3-4 days. Evidence of oophagy was categorized into three increasing levels: Individuals that were observed to handle embryo masses but not consume them provided the weakest evidence of oophagy; embryo masses that were found damaged but were not directly observed to be eaten; and direct observations of handling and consumption of embryo masses.

Family	Species	Witnessed handling	Found damaged	Witnessed consuming	Total
Porcellanidae	*Petrolisthes eriomerus*	0	2	0	2 of 4
Epialtidae	*Pugettia gracilis*	0	2	0	2 of 4
Epialtidae	*Pugettia producta*	0	3	0	3 of 4
Grapsidae	*Hemigrapsus oregonensis*	0	1	0	1 of 1
Grapsidae	*Hemigrapsus nudus*	0	0	0	0 of 4
Hippolytidae	*Heptacarpus brevirostris*	0	3	1	4 of 4
Muricidae	*Nucella lamellosa*	0	0	0	0 of 4

Hermissenda crassicornis hatching plasticity experiment

To investigate if *H. crassicornis* modify hatch timing in response to chronic chemical

cues from predators and/or acute mechanical disruption of the embryo mass, I employed a fully

crossed factorial design. I measured the time-to-hatching for each embryo mass using my

customized hatching detectors. The chemical cue factor had three levels: no cue (control),

predator cue (from *H. brevirostris*), and non-predator cue (*P. eriomerus*). The mechanical cue

factor had two levels: no disruption (control), and disruption of the embryo mass seven days after

oviposition using forceps. I performed this experiment between Nov 11th and Dec 26th 2017.

I collected *H. crassicorni*s as well as *Mytilus edulis*, *Obelia dichotoma* and other

associated fouling species from the docks of the Anacortes Marina and kept them in a single

aquarium. *H. crassicornis* grazed on the *O. dichotoma*, but I also fed them shelled *M. edulis*. I

checked for newly oviposited embryo masses every 3 hours between 6:00 AM and midnight (i.e.,

no checks were performed at 3:00 AM), collected any embryo masses that were completely

oviposited and recorded the date and time. The *H. crassicornis* embryo masses were easily

removed from the walls or bottom of the aquaria using a razor blade. However, in most cases, the

embryo masses were oviposited on stalks of *O. dichotoma*, in which case I trimmed the stalks

and carefully extracted them from the embryo masses using forceps with the aid of a dissecting

microscope and chilled watch glass. I took great care in removing as much *O. dichotoma* as

possible without causing damage to the embryo masses. Although the stolons were typically easy

to extract, I occasionally left portions of the perisarcs that were deeply embedded inside the

embryo masses that were too risky to be removed without damaging the embryo mass. I then

placed the cleaned embryo masses inside GA-7 Magenta vessels (77mm x 77mm x 97 mm) filled

with 45 μm vacuum-filtered Shannon Point seawater (FSW) aerated by bubble stones and left

them to incubate in the cold room prior to assigning them to treatments.

I collected *H. brevirostris* (1.72 ± 0.29 SE g wet mass) from the docks of Anacortes

Marina and *P. eriomerus* (2.55 ± 0.14 SE g wet mass) from the rocky, low intertidal near the

Shannon Point Marine Center, and kept species in separate aquaria in the cold room. I fed the *H.*

brevirostris with shelled *M. edulis* and the *P. eriomerus* filter fed directly from the raw seawater.

I placed a divider in these aquaria so that I would be able to separate fed specimens from starved

specimens. The crab and shrimp specimens starved when placed in the treatment aquaria of the

hatching plasticity experiment, so the divider allowed me to rotate the starved specimens with

recently fed specimens every four days.

To determine if *H. crassicornis* larvae modify hatch timing in response to mechanical

cues, I disrupted the outer envelope of a subset of embryo masses using forceps to simulate

predator attacks. Although *H. crassicornis* veligers hatch 5-6 days after oviposition at 13-15 º C

(Harrigan & Alkon 1978) or 7-days after at 14 ºC (Williams 1980), I observed hatching

approximately 9-10 days after oviposition at 10-12 ºC. *P. sibogae* veligers were shown to hatch

7-11 days after oviposition when embryo masses were left undisturbed, but as soon as 4 days

after oviposition when disturbed (Strathmann et al. 2010). To limit the number of levels of the

mechanical cue factor to two so I could increase the number of replicates, I chose to either leave

embryo masses undisturbed (control) or simulate predatory attacks seven days after oviposition

as it is considerably sooner than nine days but also not likely earlier than when the developing

veligers gain swimming competence (Strathmann et al. 2010).

To investigate interactive effects of the mechanical cues and chemical cues, I employed a

fully crossed experimental design with 6 treatments. Hereafter I will refer to these treatments in

order of *mechanical x chemical* cue, with the levels 'control' and 'attack' for the mechanical

cues and 'control', 'non-predator', and 'predator' for the chemical cues.

I prepared 36 replicate aquaria arranged in 3 rows and 12 columns in the water table,

each with an embryo mass hatching detector equipped with infrared sensors for detecting

hatching activity (Figure 2.3) and filled with 1.0 L FSW. The laboratory's fluorescent lights were

mostly kept at a 12-hour light/dark cycle, with the except that the lights were turned on during

brief checks during the dark period. Using a randomized unreplicated block design, where each

block consisted of 6 aquaria arranged in 3-rows and 2-columns, I assigned one replicate of each

of the six treatments to each block using a random number generator. The spatial block design

allowed me to account for random effects, such as temperature gradients in the water table. I

placed embryo masses into randomly assigned treatment aquaria 0.75-1.25 days after deposition.

Therefore, replicates were gradually set up as the parent nudibranchs oviposited successive

clutches. Every four days, I replaced 50% of the FSW in each container and rotated the starved

shrimp and crab specimens in the treatments with fed specimens so that they would release

kairomones in the treatments and to prevent animals from starving to death. I monitored hatching

activity of the embryo masses several times every day (e.g., Figure 2.4) and waited 4-5 days after

hatching was first detected before cleaning and resetting treatment aquaria for subsequent

replicates. Most sensors were used for 2 replicates. Embryo masses that were oviposited between

Nov 11th and Nov 20th, 2017 were in the first batch and those between Nov 28th and Dec 11th

were in the second batch.

The experiment ran for 39 days, during which 67 embryo masses were monitored under

treatments. However, 17 embryo masses failed to hatch, resulting in time-to-hatching estimates

for only 50 embryo masses. Some hatching failure was expected but not quite to this degree, and possible reasons will be discussed later. As a result, the treatments had between 7-10 replicates.

Onchidoris bilamellata hatching plasticity experiment

In the second hatching plasticity experiment, I investigated the hatch timing of *O. bilamellata* embryo masses in response to chronic exposure to chemical cues from an embryo mass predator, the stout shrimp *H. brevirostris*, and a non-predator snail, *N. lamellosa*, relative to a control treatment (no chemical cues). I opted to not cross the chemical cue factor with a mechanical cue factor because *O. bilamellata* were more difficult to find later in the breeding season. Additionally, I quantified time-to-hatching using my custom IR hatch timing sensors, but several sensors stopped functioning after the first experiment, which limited sample size compared to the first experiment. With the exception of excluding the mechanical factor and the species representing the chemical factor levels, the *O. bilamellata* hatching plasticity experiment was conducted with the same protocols as the first experiment. With three treatments, there were twelve spatial blocks in the water table. I performed this experiment between Feb 21 and Mar 22, 2018.

I collected *O. bilamellata* and *H. brevirostris* from the docks of Anacortes Marina and *N. lamellosa* from the rocky, low intertidal of Port of Bellingham Marine Park, and kept them in separate aquaria in the cold room. I fed shelled *M. edulis* to the *H. brevirostris*, and shelled *M. edulis* and barnacles to the *N. lamellosa*.

This experiment ran for 29 days, during which the hatch timing of 19 *O. bilamellata* embryo masses was monitored. Two embryo masses failed to hatch and one sensor failed to provide an accurate timing estimate due to a malfunction, resulting in time-to-hatching estimates

for 16 embryo masses. Unfortunately, the 2 failed embryo masses were both within the non-predator treatment, so the replicates were unbalanced between the treatments (control: n = 6; non-predator: n = 4; predator: n = 6).

Analyses

I analyzed differences in time-to-hatching between treatments using linear mixed-effects models with a random block effect. The fixed-effects in the *H. crassicornis* PIHP experiment were both the physical and chemical factors fully-crossed. In the *O. bilamellata* PIHP experiment, the chemical factor was the only fixed effect. The random effect of the aquaria blocks was included in all models because of the experimental design to account for any spatial variability (e.g. temperature) in the water table.

I estimated time-to-hatching of the embryo masses by de-noising and performing breakpoint analyses on the hatching activity data in R (R Core Team 2019). I first removed data from faulty emitter/phototransistors (identified by moving mean values that were static at maximum or minimum values), removed outliers, scaled the exponentially weighted moving variance values, applied smoothers, and averaged the observations from the sensor arrays. I then performed breakpoint analyses on these simplified datasets using the *CE.Normal.MeanVar* function from the *breakpoint* package (Priyadarshana & Sofronov 2016) parameterized to find a single breakpoint. I calculated the time-to hatching (incubation duration) as the time difference between the time of hatching and the time of oviposition.

All analyses were performed in R version 3.6.1 (R Core Team 2019). I built linear mixed-effects models using the *lmer* function from the *lmerTest* package which uses Satterthwaite's method to provide p-values for ANOVA tables. I used the model:

$$T_{ijkl} = \mu + C_i + M_j + (CM)_{ij} + \beta_{(ij)k} + \epsilon_{ijkl}$$

for the *H. crassicornis* hatching plasticity experiment and

$$T_{ijk} = \mu + C_i + \beta_{(i)j} + \epsilon_{ijk}$$

for the *O. bilamellata* hatching plasticity experiment, where T = time to hatching in days, C = chemical cue factor, M = mechanical cue factor, and β = aquaria block as a random intercept. The control level of the chemical cue and the undisturbed level of the mechanical cue were set as the baselines.

I checked model assumptions for normality of residuals, homogeneity of variance, and non-autocorrelation. In the *H. crassicornis* hatching plasticity experiment, residuals were normally distributed according to the Shapiro-Wilk normality test ($W = 0.97$, $p = 0.17$) and a quantile-quantile plot also indicated normality. However, Levene's test indicated that the assumption of homogeneity of variance was violated ($F = 2.70$, df1 = 5, df2 = 44, $p = 0.03$). Moreover, plotting the residuals in chronological order indicated autocorrelation. To account for this temporal trend in hatch timing, embryo mass batch (as either first or second batch) was added to the linear mixed-effects model as a fixed effect (B) and as an interaction with the mechanical factor (MB), resulting in the revised model:

$$T_{ijklm} = \mu + C_i + M_j + (CM)_{ij} + B_k + (MB)_{jk} + \beta_{(ijk)l} + \epsilon_{ijklm}.$$

This revised model passed the Shapiro-Wilk normality test ($W = 0.97$, $p = 0.21$) and Levene's test ($F = 0.34$, df1 = 11, df2 = 38m, $p = 0.97$), and diagnostic plots indicated no autocorrelation. All other possible models including B or its interactions failed tests of assumptions. In the *O. bilamellata* hatching plasticity experiment, residuals were normally distributed ($W = 0.97$, $p = 0.83$) and variances were homogenous across groups ($F = 1.55$, df1 = 2, df2 = 13, $p = 0.25$).

Results

Hermissenda crassicornis **hatching plasticity experiment**

There was a significant interaction between the mechanical factor and embryo mass batch on time-to-hatching of *H. crassicornis* embryo masses (Table 3.3, $p < 0.001$). Neither the chemical cue nor its interaction with the mechanical cue had a significant effect on hatch timing. The fitted model attributed no variation to the spatial block. Average time-to-hatching was 9.60 days (Figure 3.2, n = 50, SE = 0.23). Embryo masses that were attacked (mean = 9.32 d, n = 28, SE = 0.37) hatched 6.42% faster on average than those left intact (mean = 9.95 d, n = 22, SE = 0.20). Embryo masses in the first batch (mean = 10.7 d, n = 27, SE = 0.181) hatched 22.5% faster than those in the second batch (mean = 8.30 d, n = 23, SE = 0.262). Among the embryo masses that were undisturbed, those in the first batch hatched after 10.48 days (n = 12, SE = 0.212) whereas those in the second batch hatched 11.0% faster, after 9.32 days (n = 10, SE = 0.258). However, among the embryo masses that were attacked, those in the first batch hatched after 10.9 days (n = 12, SE = 0.276) whereas those in the second batch hatched 44.9% faster, after 7.51 days (n = 13, SE = 0.257). Therefore, time-to-hatching was lower in the second batch compared to the first batch and the simulated predator attack further accelerated time-to-hatching of embryos in the second batch.

Table 3.3. Linear mixed-effects model with block as a random intercept of hatch timing of *Hermissenda crassicornis* embryo masses in response to chemical cues from predator and non-predators and/or mechanical cues via simulated predator attack involving disruption of the embryo mass outer envelope, split by embryo mass batch (first or second). This analysis was performed post-hoc following the observations that embryo masses in the second batch hatched sooner on average than those in the first batch and even more so when attacked.

Source of variation	Sum Sq	Mean Sq	NumDF	DenDF	F	p-value
Mechanical	6.19	6.19	1	42	7.50	**0.009**
Chemical	2.99	1.49	2	42	1.81	0.176
Batch	61.66	61.66	1	42	74.67	**< 0.001**
Mechanical x Chemical	0.38	0.19	2	42	0.23	0.795
Mechanical x Batch	15.54	15.54	1	42	18.83	**< 0.001**
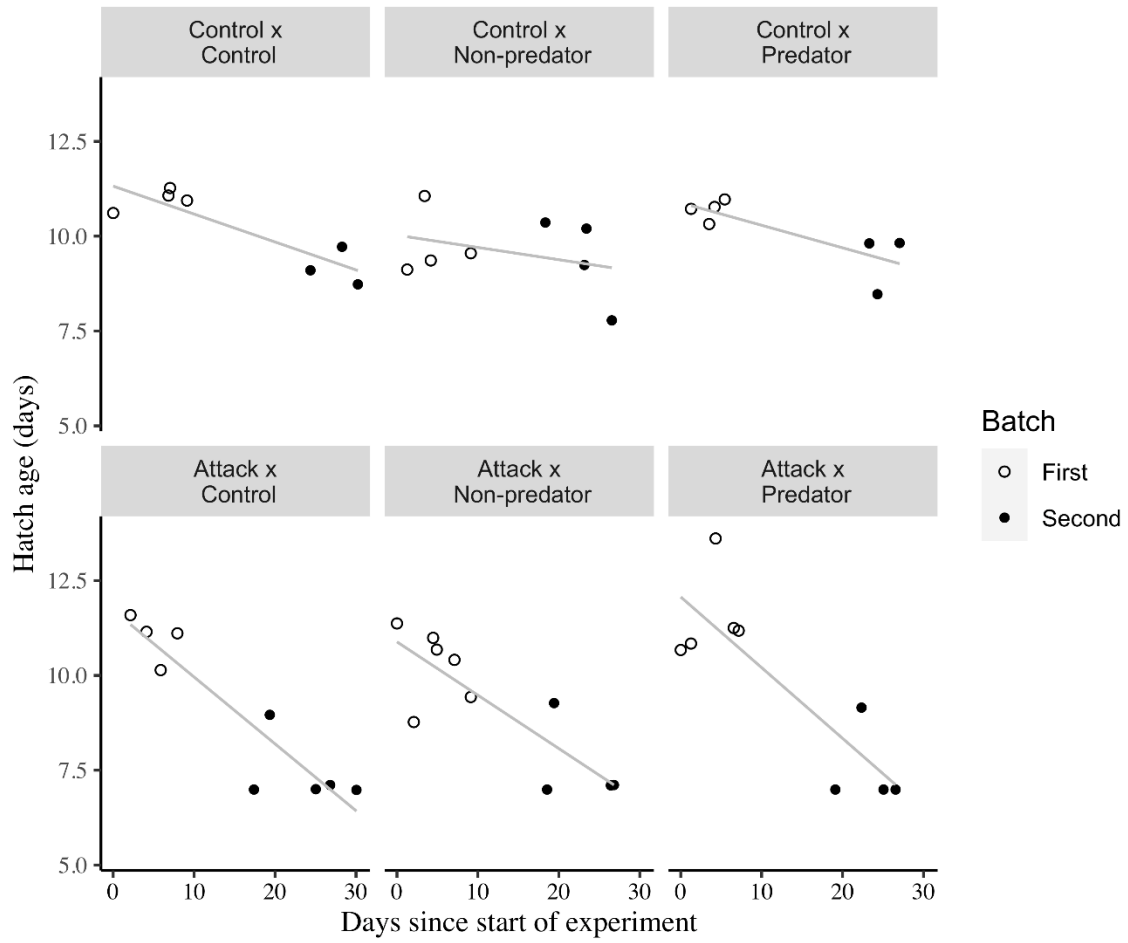
Figure 3.2. Time from oviposition to first hatching for *Hermissenda crassicornis* over the elapsed duration of the hatching plasticity experiment, with fitted linear models represented by gray lines and batches represented by unfilled (first) and filled (second) points.

Onchidoris bilamellata hatching plasticity experiment

There was no significant effect of the chemical treatments on time-to-hatching of *O. bilamellata* embryo masses (Table 3.4, Figure 3.3). Embryo masses hatched after 11.52 days on average (n = 16, SE = 0.38). The non-predator chemical cue treatment had the lowest average time-to-hatching of 10.58 days (n = 4, SE = 0.73), which was 12.17% less than the treatment with the highest average time-to-hatching of 12.05 days (n = 6, SE = 0.83). The predator chemical cue treatment was intermediate with an average time-to-hatching of 11.63 days (n = 6, SE = 0.28).

Following the discovery of the apparent effect of time and batch on hatch timing in the *H. crassicornis* hatching plasticity experiment, I also checked to see if a similar pattern existed with *O. bilamellata*. Since there was only one batch of embryo masses, the experiment had a shorter duration than the *H. crassicornis* experiment. Within both the control and non-predator chemical cue treatments, time-to-hatching decreased over the course of the experiment, similar to all treatments in the *H. crassicornis* hatching plasticity experiment. The predator chemical cue treatment differed in that time-to-hatching was weakly positively correlated with the duration of the experiment (Figure 3.4).

Table 3.4. Linear mixed-effects model with block as a random intercept of hatch timing of *Onchidoris bilamellata* embryo masses in response to chemical cues from predator and non-predators.

Source of variation	Sum Sq	Mean Sq	NumDF	DenDF	F	p-value
Chemical	2.36	1.18	2	5.94	0.89	0.46
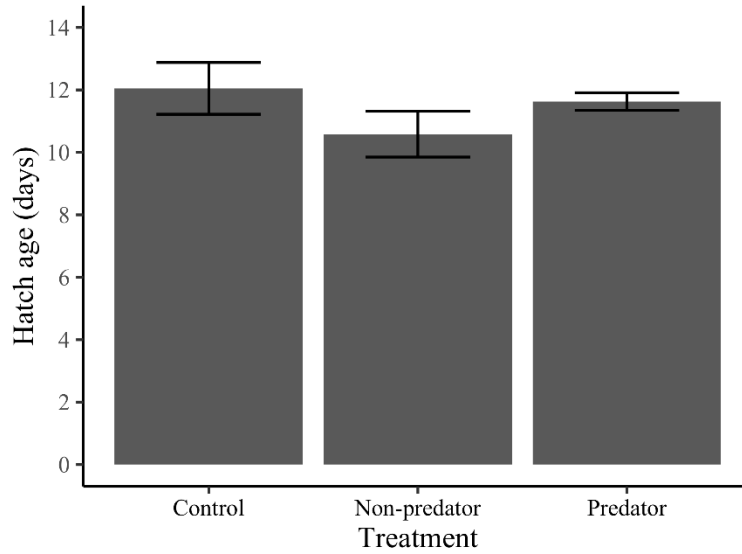
Figure 3.3. Time from oviposition to first hatching of nudibranch *Onchidoris bilamellata* embryo masses in response to chemical cues: control (no cues), cues from non-predatory snail *Nucella lamellosa*, and cues from a predatory shrimp *Heptacarpus brevisrostris*. Error bars represent standard error.
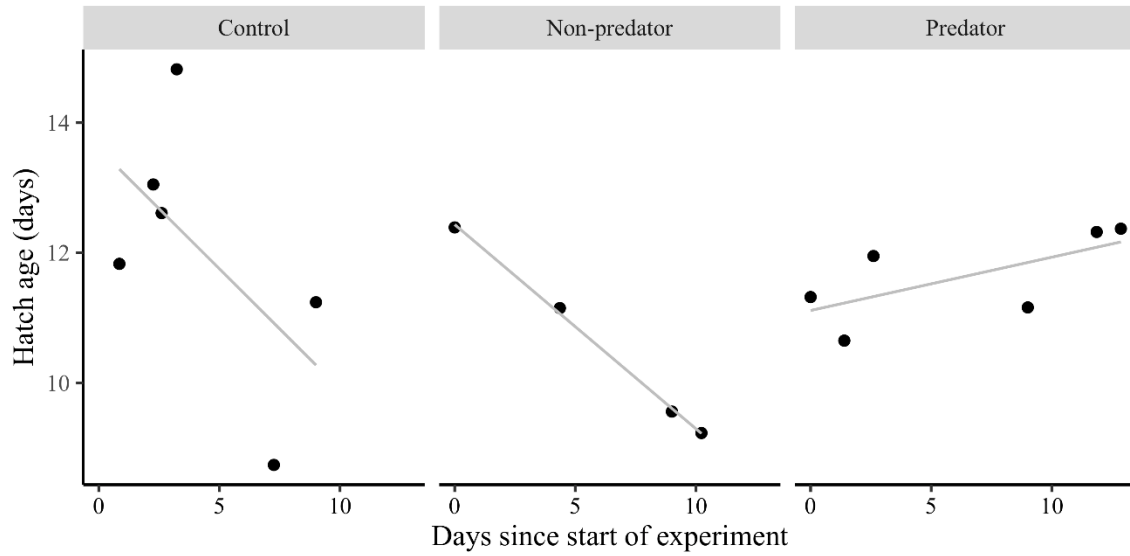
Figure 3.4. Time from oviposition to first hatching for *Onchidoris bilamellata* versus the elapsed

duration the hatching plasticity experiment, with fitted linear models represented by gray lines.

Discussion

Although the hypothesized interaction between the mechanical and chemical cues was not observed, I did find evidence that mechanical disruption of the embryo mass can decrease time-to-hatching of *H. crassicornis* embryos. This effect was only observed for embryos in the second of two batches, which also hatched sooner regardless of the experimental treatments. Other PIHP studies observed 50% reductions in hatch timing in response to staged (Warkentin 1995) and simulated (Strathmann et al. 2010) predator attacks, comparable to the 45% reduction of hatching timing that I observed in the second batch of *H. crassicornis* embryo masses. I did not find any significant effect of chemical cues on hatching timing in either *H. crassicornis* or *O. bilamellata,* so my hypothesis that chronic exposure of chemical cues from a predator would reduce hatch timing relative to those of a non-predator and a control treatment was not supported.

Within all experimental treatments of the *H. crassicornis* PIHP experiment, time-to-hatching decreased. The temperature of the water table was maintained constant at 12 ºC, so the decreasing time-to-hatching cannot be explained by an increased temperature over the duration of the experiment. Larvae might hatch earlier and at a smaller size when adults are starved (Chester 1996), but this explanation is also unlikely as the adult *H. crassicornis* were provided an abundance of food. It is possible that the diet I provided was more protein-rich than what is normally available *in situ* but the literature does not cite impacts of diet on embryonic duration, only on planktonic duration (Bertram & Strathmann 1998), hatching success, and survival (Guisande & Harris 1995). Increased oxygen availability can also decrease time to hatching (Eyster 1986) but there was also no difference in how the aquaria were aerated between the two batches.

One possible cause of the decreased embryonic period in the *H. crassicornis* second batch as well as the interaction between the mechanical cue and batch is that the concentration of nematodes, ciliates, copepods and other biofouling organisms in the aquarium housing the adults increased over time. These organisms are known to weaken the matrix of the embryo masses and facilitate the escape of swimming veliger larvae (Hurst 1967). Secondarily, this activity may also increase the permeability of the embryo masses to oxygen and thereby promote development and earlier hatching. Therefore, embryos in the second batch could have had been more responsive to the simulated predator attack than those in the first batch. Although embryo masses were collected within 3-hours of oviposition, it was impossible to prevent these organisms from inhabiting the embryo masses before placing them in the treatment aquaria. Additionally, these organisms could have also hitchhiked on the predator and non-predator species that were regularly swapped out every 4 days. Although I performed regular water changes on all aquaria, it was not likely to keep the population of these organisms constant over the course of the experiment. Transferring the adults to a newly cleaned tank between the batches may mitigate this potential issue, as would using separate shipments of lab-reared nudibranchs (Harrigan & Alkon 1978) or using a longer period for nudibranchs to acclimate prior to beginning hatching plasticity experiments (Barbeau 2004).

Further work is warranted to determine the age at which larvae achieve swimming and hatching competence. Rearing methods for *H. crassicornis* involve manually liberating the embryo capsules from the embryo mass 5-6 days following oviposition for embryo masses incubated at 13-15 ºC (Harrigan & Alkon 1978), which is done in a manner that is more aggressive than what I did (teasing all embryos out of the embryo mass versus tearing the outer envelope a few times). Therefore, it does not appear that the development of the veligers is

arrested by removing them completely from the matrix of the embryo mass and that they can continue to develop prior to hatching. In a scenario where an embryo mass is attacked by a predator, the developing larvae must be capable of both hatching and swimming to avoid predation. By repeating this experiment with a greater number of levels of the mechanical cue factor (e.g., simulated attack at days 3, 5, and 7, etc.), I could determine the age at which hatching competence is gained and whether the timing of disturbance to the embryo mass differentially affects hatch timing.

There are several possible explanations for why I did not observe any significant effects of the chronic chemical cues on hatch timing of either *H. crassicornis* or *O. bilamellata*. I only used *H. brevirostris* as the predator species, so it is possible that these nudibranchs do exhibit PIHP, just not to this specific predator. Because the larvae were chronically exposed to chemical cues, it is possible that they became habituated and opted to not hatch prematurely (Blumstein 2016). Perhaps, if chemical cues from predators are first detected at a later developmental stage when swimming and hatching competence is achieved, larvae perceive this as a change in predation risk and hatch prematurely. It is also possible that neither *H. crassicornis* nor *O. bilamellata* exhibit PIHP to the chemical cues I presented and instead rely on responses to mechanical cues or utilize other antipredator behaviors such as incorporating chemical defenses in embryo masses (Pawlik et al. 1998, McClintock & Baker 1997, Wood et al. 2012).

Examining predator-induced hatching plasticity within marine invertebrates is worth exploring for the additional reason that it might indirectly affect dispersal. Many newly-hatched individuals are swimming planktotrophs (Vance 1973, Strathmann 1987, Goddard 2004) and must feed for a certain period before metamorphosing into benthic adults (Hadfield & Strathmann 1996). For many of these species, this planktonic stage plays a key role in dispersal

(Palumbi 1995, Strathmann et al. 2002, Marshall et al. 2012). If time-to-hatching is plastic and is accelerated in response to high embryo-stage predation risk, the hatched planktonic larvae likely have a prolonged duration of planktonic development before metamorphic competence. Therefore, the dispersal distance of a prey species is influenced by predators (Strathmann et al. 2010, Oyarzun & Strathmann 2011).

Variability in embryonic duration

Within both hatching plasticity experiments, the time-to-hatch was quite variable, even within treatments. Even within an embryo mass, larvae will develop at different rates and gain swimming and hatching competence at different times. This strategy is believed to be a form of bet-hedging to favor dispersal and resource availability over a wider scale of time and space (Pechenik 1990, Avila 1998). Most studies summarize time to hatch observations as the mean, and those that do provide a range typically present it using ± 1 standard deviation. Among studies that do present some form of a range of embryonic duration, it is approximately 3 days (Goddard 1992). However, the full range of hatching timing observations are rarely provided. In one nearby study in Oregon, the arminacean nudibranch *Janolus fuscus* was observed to have a wide embryonic duration of 10-18 days (Wolf & Young 2012). Given the previously mentioned factors that are known to affect the duration of embryonic development (some of which are more easily controlled than others), studies such as mine require an adequate sample size to overcome the high inherent variability to detect statistically significant effects of treatments.

Hatching failure

Both of the hatch timing studies suffered diminished sample sizes because some embryos failed to hatch. Many nudibranch species can oviposit several embryo masses following a single copulation, although some, like *Onchidoris fusca*, tend to spawn only once following copulation. The proportion of unfertilized eggs within an embryo mass increases with subsequent spawnings after copulation, and Hadfield (1963) speculated that if too few embryos develop, there might be inadequate production of enzymes necessary to trigger hatching. I did take care to ensure that all embryo masses were indeed fertilized prior to placing them under treatment. During the teardown of the replicates, I noted that some embryo masses seemed to have arrested development at an early stage while others were either decomposed and/or overrun with ciliates and nematodes. Future investigators might consider using antibiotics to mitigate contamination by biofouling organisms, but as previously noted, these organisms serve a role in the natural breakdown of the embryo mass matrix, increasing oxygen availability, and hatching as well. Ensuring that all embryo masses are provided a level of contamination within this 'Goldilocks' zone over the course of embryonic development is indeed difficult. For nudibranchs, antibiotics are typically employed after hatching at the larval stage (Hadfield 1963), not at the embryonic stage.

Performance of the hatching detectors

Both hatching plasticity experiments serve as a proof of concept that the custom IR hatching detectors can provide reliable estimates of hatch timing. Graphs of the raw data collected by the sensors generally showed clear demarcations between a constant background signal followed by a sudden increase in variation at the onset of hatching. The post-processing

program consistently identified this breakpoint and was able to differentiate it from temporary disturbances (such as the simulated predator attacks or inadvertent vibrations).

I have identified several improvements to the sensors that would improve their utility. Of the 44 hatching detectors that I built, roughly 25% of them suffered significant damage from water exposure that either completely removed their ability to turn on, communicate, or reduced the number of functioning IR emitter/sensor pairs below 4 (out of 6). The bubble stones in the aquaria were tuned to provide adequate aeration without excessive splashing, but there was enough water and salt in the air to expose weaknesses in waterproofing. Although several acrylic coatings were applied to all parts of the sensors not encased in silicone, many of the sensors had visible corrosion at the soldering joints at the power leads and the wireless transmitter. An epoxy was later applied to all sensors at the points (between the first and second batch of the *H. crassicornis* experiment) that fairly effectively prevented further sensor failures. In terms of the on-board data processing (calculations of moving mean and variance) and post-processing (detecting signal from noise), there are two key improvements to be made. I designed the sensors with the goal of identifying time of first hatching, but hatching within an embryo mass is not uniform. If I had calibrated each sensor to known densities of larvae, I could have estimated not only the time of first hatching, but also characterized the distribution of hatch timing for all hatched larvae. For instance, chemical cues might have an effect on time of first hatching but instead have a noticeable effect on the mean time of hatching.

Works Cited

Adler, F.R., and Harvell, C.D. (1990). Inducible defenses, phenotypic variability and biotic environments. Trends in Ecology & Evolution 5, 407–410.

Agrawal, A.A. (2001). Phenotypic plasticity in the interactions and evolution of species. Science 294, 321–326.

Alkon, D.L. (1983). Learning in a Marine Snail. Sci Am 249, 70–84.

Armstrong, A.F., Blackburn, H.N., Allen, J.D., Tewksbury, N.H.E.J., and McPeek, E.M.A. (2013). A Novel Report of Hatching Plasticity in the Phylum Echinodermata. The American Naturalist 181, 264–272.

Austin, R.W., and Halikas, G. (1980). The index of refraction of seawater. SIO Ref. No. 76-1, Scripps Institution of Oceanography. San Diego, California.

Avila, C., Grenier, S., Tamse, C.T., and Kuzirian, A.M. (1997). Biological factors affecting larval growth in the nudibranch mollusc *Hermissenda crassicornis* (Eschscholtz, 1831). Journal of Experimental Marine Biology and Ecology 218, 243–262.

Avila, C., Tyndale, E., and Kuzirian, A.M. (1998). Feeding behavior and growth of *Hermissenda crassicornis* (mollusca: Nudibranchia) in the laboratory. Marine and Freshwater Behaviour and Physiology 31, 1–19.

Barbeau, M.A., Durelle, K., and Aiken, R.B. (2004). A design for multifactorial choice experiments: an example using microhabitat selection by sea slugs Onchidoris bilamellata (L.). Journal of Experimental Marine Biology and Ecology 307, 1–16.

Benard, M.F. (2004). Predator-induced phenotypic plasticity in organisms with complex life histories. Annu. Rev. Ecol. Evol. Syst. 35, 651–673.

Bertram, D.F., and Strathmann, R.R. (1998). Effects of maternal and larval nutrition on growth and form of planktotrophic larvae. Ecology 79, 315–327.

Bleakney, J., and Saunders, C. (1978). Life history observations on nudibranch mollusk *Onchidoris bilamellata* in intertidal zone of Nova Scotia. Can. Field Nat. 92, 82–85.

Blumstein, D.T. (2016). Habituation and sensitization: new thoughts about old ideas. Animal Behaviour 120, 255–262.

Bourdeau, P.E., and Padilla, D.K. (2019). Cue specificity of predator-induced phenotype in a marine snail: is a crab just a crab? Marine Biology 166, 84.

Bradshaw, A.D. (1965). Evolutionary significance of phenotypic plasticity in plants. Advances in Genetics 13, 115–155.

Brooks, W.R., and Mariscal, R.N. (1986). Population variation and behavioral changes in two pagurids in association with the sea anemone *Calliactis tricolor* (Lesueur). Journal of Experimental Marine Biology and Ecology 103, 275–289.

Chang, E.S. (2014). Possible anti-predation properties of the egg masses of the marine gastropods *Dialula sandiegensis*, *Doris montereyensis* and *Haminoea virescens* (Mollusca, Gastropoda).

Chester, C.M. (1996). The effect of adult nutrition on the reproduction and development of the estuarine nudibranch, *Tenellia adspersa* (Nordmann, 1845). Journal of Experimental Marine Biology and Ecology 198, 113–130.

Chia, F.-S., and Koss, R. (1988). Induction of settlement and metamorphosis of the veliger larvae of the nudibranch, Onchidoris bilamellata. International Journal of Invertebrate Reproduction and Development 14, 53–69.

Chivers, D.P., Kiesecker, J.M., Marco, A., Devito, J., Anderson, M.T., and Blaustein, A.R. (2001). Predator-induced life history changes in amphibians: egg predation induces hatching. Oikos 92, 135–142.

Claverie, T., and Kamenos, N.A. (2008). Spawning aggregations and mass movements in subtidal *Onchidoris bilamellata* (Mollusca: Opisthobranchia). Journal of the Marine Biological Association of the United Kingdom 88, 157–159.

Cohen, C.S., and Strathmann, R.R. (1996). Embryos at the edge of tolerance: effects of environment and structure of egg masses on supply of oxygen to embryos. The Biological Bulletin 190, 8–15.

Crane, S. (1971). The feeding and reproductive behavior of the sacoglossan gastropod *Olea hansineensis* Agersborg, 1923. Veliger 14, 57–59.

De Roeck, E.R., Artois, T., and Brendonck, L. (2005). Consumptive and non-consumptive effects of turbellarian (*Mesostoma* sp.) predation on anostracans. In Aquatic Biodiversity II, (Springer), pp. 103–111.

DeWitt, T.J. (1998). Costs and limits of phenotypic plasticity: Tests with predator-induced morphology and life history in a freshwater snail. Journal of Evolutionary Biology 11, 465–480.

DeWitt, T.J., Sih, A., and Wilson, D.S. (1998). Costs and limits of phenotypic plasticity. Trends in Ecology & Evolution 13, 77–81.

Dodson, S. (1989). Predator-induced reaction norms. Bioscience 39, 447–452.

Donohue, K. (2002). Germination timing influences natural selection on life-history characters in *Arabidopsis thaliana*. Ecology 83, 1006–1016.

Eyster, L.S. (1983). Ultrastructure of early embryonic shell formation in the opisthobranch gastropod *Aeolidia papillosa*. The Biological Bulletin 165, 394–408.

Fordyce, J.A. (2006). The evolutionary consequences of ecological interactions mediated through phenotypic plasticity. Journal of Experimental Biology 209, 2377–2383.

Fusco, G., and Minelli, A. (2010). Phenotypic plasticity in development and evolution: facts and concepts. Philosophical Transactions of the Royal Society of London B: Biological Sciences 365, 547–556.

Gibson, G.D. (1997). Variable Development in the Spionid *Boccardia proboscidea* (Polychaeta) Is Linked to Nurse Egg Production and Larval Trophic Mode. Invertebrate Biology 116, 213–226.

Goddard, J.H.R. (1992). Patterns of development in nudibranch mollusks from the northeast Pacific Ocean, with regional comparisons. PhD Thesis. Thesis (Ph. D.)–University of Oregon, 1992.

Goddard, J.H. (2004). Developmental mode in benthic opisthobranch molluscs from the northeast Pacific Ocean: feeding in a sea of plenty. Canadian Journal of Zoology 82, 1954–1968.

Gosselin, L.A. (1997). An ecological transition during juvenile life in a marine snail. Marine Ecology Progress Series 157, 185–194.

Gotshall, D.W., Laurent, L.L. (1980). Pacific Coast Subtidal Marine Invertebrates. Sea Challengers, Monterey, CA.

Guisande, C., and Harris, R. (1995). Effect of total organic content of eggs on hatching success and naupliar survival in the copepod Calanus helgolandicus. Limnology and Oceanography 40, 476–482.

Hadfield, M.G. (1963). The Biology of Nudibranch Larvae. Oikos 14, 85–95.

Hadfield, M., and Strathmann, M. (1996). Variability, flexibility and plasticity in life histories of marine invertebrates. Oceanologica Acta 19, 323–334.

Harmon, E.A., and Allen, J.D. (2018). Predator-induced plasticity in egg capsule deposition in the mud snail *Tritia obsoleta*. Marine Ecology Progress Series 586, 113–125.

Harrigan, J.F., and Alkon, D.L. (1978). Larval rearing, metamorphosis, growth and reproduction of the eolid nudibranch *Hermissenda crassicornis* (Eschscholtz, 1831)(Gastropoda: Opisthobranchia). Biological Bulletin 154, 430–439.

Harvell, C.D. (1986). The ecology and evolution of inducible defenses in a marine bryozoan: cues, costs, and consequences. The American Naturalist 128, 810–823.

Harvell, C.D. (1990). The ecology and evolution of inducible defenses. The Quarterly Review of Biology 65, 323–340.

Harvell, C.D. (1992). Inducible defenses and allocation shifts in a marine bryozoan. Ecology 73, 1567–1576.

Hoverman, J.T., Auld, J.R., and Relyea, R.A. (2005). Putting prey back together again: integrating predator-induced behavior, morphology, and life history. Oecologia 144, 481–491.

Huber, H., Kane, N.C., Heschel, M.S., von Wettberg, E.J., Banta, J., Leuck, A.-M., and Schmitt, J. (2004). Frequency and microenvironmental pattern of selection on plastic shade-avoidance traits in a natural population of *Impatiens capensis*. The American Naturalist 163, 548–563.

Hurst, A. (1967). The egg masses and veligers of thirty northeast Pacific opisthobranchs. Veliger 9, 255–288.

Kimirei, I.A., Nagelkerken, I., Trommelen, M., Blankers, P., Van Hoytema, N., Hoeijmakers, D., Huijbers, C.M., Mgaya, Y.D., and Rypel, Al. (2013). What drives ontogenetic niche shifts of fishes in coral reef ecosystems? Ecosystems 16, 783–796.

Knudsen, J.W. (1964). Observations of the reproductive cycles and ecology of the common Brachyura and crablike Anomura of Puget Sound, Washington.

Li, D. (2002). Hatching responses of subsocial spitting spiders to predation risk. Proceedings of the Royal Society of London B: Biological Sciences 269, 2155–2161.

Lindsay, T., and Valdés, Á. (2016). The model organism *Hermissenda crassicornis* (Gastropoda: Heterobranchia) is a species complex. PLOS ONE 11, e0154265.

Marshall, D.J., Krug, P.J., Kupriyanova, E.K., Byrne, M., and Emlet, R.B. (2012). The biogeography of marine invertebrate life histories. Annual Review of Ecology, Evolution, and Systematics 43, 97.

McClintock, J.B., and Baker, B.J. (1997). Palatability and chemical defense of eggs, embryos and larvae of shallow-water Antarctic marine invertebrates. Marine Ecology Progress Series 121–131.

McCormick, L.R., Levin, L.A., and Oesch, N.W. (2019). Vision is highly sensitive to oxygen availability in marine invertebrate larvae. Journal of Experimental Biology 222.

Megina, C., Gosliner, T., and Cervera, J.L. (2007). The use of trophic resources by a generalist eolid nudibranch: Hermissenda crassicornis (Mollusca : Gastropoda). Cah. Biol. Mar. 48, 1–7.

Millen, Sandra V., F. (1980). Range extensions, new distribution sites, and notes on the biology of sacoglossan opisthobranchs (Mollusca: Gastropoda) in British Columbia. Can. J. Zool. 58, 1207–1209.

Miller, S.E., and Hadfield, M.G. (1986). Ontogeny of phototaxis and metamorphic competence in larvae of the nudibranch *Phestilla sibogae* Bergh (Gastropoda: Opisthobranchia). Journal of Experimental Marine Biology and Ecology 97, 95–112.

Miner, B.G., Donovan, D.A., and Andrews, K.E. (2010). Should I stay or should I go: predator- and conspecific-induced hatching in a marine snail. Oecologia 163, 69–78.

Moran, A.L., and Woods, H.A. (2007). Oxygen in egg masses: interactive effects of temperature, age, and egg-mass morphology on oxygen supply to embryos. Journal of Experimental Biology 210, 722–731.

Orians, G.H., and Janzen, D.H. (1974). Why are embryos so tasty? The American Naturalist 108, 581–592.

Orizaola, G., Dahl, E., and Laurila, A. (2012). Reversibility of predator-induced plasticity and its effect at a life-history switch point. Oikos 121, 44–52.

Oyarzun, F.X., and Strathmann, R.R. (2011). Plasticity of hatching and the duration of planktonic development in marine invertebrates. Integrative and Comparative Biology 51, 81–90.

Palumbi, S.R. (1995). Using genetics as an indirect estimator of larval dispersal (Boca Raton, FL: CRC Press).

Pawlik, J.R., Kernan, M.R., Molinski, T.F., Harper, M.K., and Faulkner, D.J. (1988). Defensive chemicals of the Spanisch dancer nudibranch *Hexabranchus sanguineus* and its egg ribbons: macrolides derived from a sponge diet. Journal of Experimental Marine Biology and Ecology 119, 99–109.

Pechenik, J.A. (1979). Role of encapsulation in invertebrate life histories. American Naturalist 859–870.

Pechenik, J.A. (1986). The encapsulation of eggs and embryos by mollusks - an overview. American Malacological Bulletin 4, 165–172.

Pechenik, J.A. (1990). Delayed metamorphosis by larvae of benthic marine invertebrates: does it occur? Is there a price to pay? Ophelia 32, 63–94.

Pfennig, D.W., Wund, M.A., Snell-Rood, E.C., Cruickshank, T., Schlichting, C.D., and Moczek, A.P. (2010). Phenotypic plasticity's impacts on diversification and speciation. Trends in Ecology & Evolution 25, 459–467.

Poo, S., and Bickford, D.P. (2014). Hatching plasticity in a Southeast Asian tree frog. Behavioral Ecology and Sociobiology 68, 1733–1740.

Potts, G.W. (1981). The anatomy of respiratory structures in the dorid nudibranchs, *Onchidoris bilamellata* and *Archidoris pseudoargus*, with details of the epidermal glands. Journal of the Marine Biological Association of the United Kingdom 61, 959–982.

Priyadarshana W.J.R.M. and Georgy Sofronov (2016). breakpoint: An R Package for Multiple Break-Point Detection via the Cross-Entropy Method. R package version 1.2. https://CRAN.R-project.org/package=breakpoint

R Core Team (2019). R: A language and environment for statistical computing. R Foundation for Statistical Computing, Vienna, Austria. ISBN 3-900051-07-0, URL http://www.R-project.org/.

Rhoades, D.F. (1985). Offensive-defensive interactions between herbivores and plants: their relevance in herbivore population dynamics and ecological theory. The American Naturalist 125, 205–238.

Rudolf, V.H., and Rasmussen, N.L. (2013). Population structure determines functional differences among species and ecosystem processes. Nature Communications 4, 1–7.

Rutowski, R.L. (1983). Mating and egg mass production in the aeolid nudibranch *Hermissenda crassicornis* (Gastropoda: Opisthobranchia). The Biological Bulletin 165, 276–285.

Scheiner, S.M. (1993). Genetics and Evolution of Phenotypic Plasticity. Annual Review of Ecology and Systematics 24, 35–68.

Sih, A., and Moore, R.D. (1993). Delayed hatching of salamander eggs in response to enhanced larval predation risk. The American Naturalist 142, 947–960.

Smith, G.R., and Fortune, D.T. (2009). Hatching plasticity of wood frog (*Rana sylvatica*) eggs in response to mosquitofish (*Gambusia affinis*) cues. Herpetological Conservation and Biology 4, 43–47.

Strathmann, M.F. (1987). Reproduction and development of marine invertebrates of the northern Pacific coast: data and methods for the study of eggs, embryos, and larvae (University of Washington Press).

Strathmann, R.R., and Chaffee, C. (1984). Constraints on egg masses. II. Effect of spacing, size, and number of eggs on ventilation of masses of embryos in jelly, adherent groups, or thin-walled capsules. Journal of Experimental Marine Biology and Ecology 84, 85–93.

Strathmann, R.R., Hughes, T.P., Kuris, A.M., Lindeman, K.C., Morgan, S.G., Pandolfi, J.M., and Warner, R.R. (2002). Evolution of local recruitment and its consequences for marine populations. Bulletin of Marine Science 70, 377–396.

Strathmann, R.R., Fenaux, L., Sewell, A.T., and Strathmann, M.F. (1993). Abundance of food affects relative size of larval and postlarval structures of a molluscan veliger. The Biological Bulletin 185, 232–239.

Strathmann, R.R., Strathmann, M.F., Ruiz-Jones, G., and Hadfield, M.G. (2010). Effect of plasticity in hatching on duration as a precompetent swimming larva in the nudibranch *Phestilla sibogae*. Invertebrate Biology 129, 309–318.

Subalusky, A.L., Fitzgerald, L.A., and Smith, L.L. (2009). Ontogenetic niche shifts in the American Alligator establish functional connectivity between aquatic systems. Biological Conservation 142, 1507–1514.

Todd, C.D. (1981). The ecology of nudibranch molluscs. Oceanography and Marine Biology: an Annual Review 17, 141-234.

Todd, C.D., and Doyle, R.W. (1981). Reproductive strategies of marine benthic invertebrates: a settlement-timing hypothesis. Marine Ecology Progress Series.

Tollrian, R., and Laforsch, C. (2006). Linking predator kairomones and turbulence: synergistic effects and ultimate reasons for phenotypic plasticity in *Daphnia cucullata*. Archiv Für Hydrobiologie 167, 135–146.

Touchon, J.C., Gomez-Mestre, I., and Warkentin, K.M. (2006). Hatching plasticity in two temperate anurans: responses to a pathogen and predation cues. Canadian Journal of Zoology 84, 556–563.

Vance, R.R. (1973). On reproductive strategies in marine benthic invertebrates. American Naturalist 339–352.

Vonesh, J.R. (2005). Egg predation and predator-induced hatching plasticity in the African reed frog, *Hyperolius spinigularis*. Oikos 110, 241–252.

Vonesh, J.R., and Bolker, B.M. (2005). Compensatory larval responses shift trade-offs associated with predator-induced hatching plasticity. Ecology 86, 1580–1591.

Warkentin, K.M. (1995). Adaptive plasticity in hatching age: a response to predation risk trade-offs. Proceedings of the National Academy of Sciences 92, 3507–3510.

Warkentin, K.M. (2002). Hatching timing, oxygen availability, and external gill regression in the tree frog, *Agalychnis callidryas*. Physiological and Biochemical Zoology 75, 155–164.

Warkentin, K.M. (2005). How do embryos assess risk? Vibrational cues in predator-induced hatching of red-eyed treefrogs. Animal Behaviour 70, 59–71.

Warkentin, K.M. (2007). Oxygen, gills, and embryo behavior: mechanisms of adaptive plasticity in hatching. Comparative Biochemistry and Physiology Part A: Molecular & Integrative Physiology 148, 720–731.

Warkentin, K.M. (2011). Environmentally cued hatching across taxa: embryos respond to risk and opportunity. Integrative and Comparative Biology 51, 14–25.

Werner, E.E., and Gilliam, J.F. (1984). The ontogenetic niche and species interactions in size-structured populations. Annual Review of Ecology and Systematics 15, 393–425.

Werner, E.E. (1986). Amphibian Metamorphosis: Growth Rate, Predation Risk, and the Optimal Size at Transformation. The American Naturalist 128, 319–341.

West-Eberhard, M.J. (1989). Phenotypic plasticity and the origins of diversity. Annual Review of Ecology and Systematics 20, 249–278.

Whitman, D.W., and Agrawal, A.A. (2009). What is phenotypic plasticity and why is it important. Phenotypic Plasticity of Insects 10, 1–63.

Williams, L.G. (1980). Development and feeding of larvae of the nudibranch gastropods *Hermissenda crassicornis* and *Aeolidia papillosa*. Malacologia 20, 99–116.

Wolf, M., and Young, C.M. (2012). Complete development of the northeast Pacific Arminacean nudibranch *Janolus fuscus*. The Biological Bulletin 222, 137–149.

Wood, S.A., Casas, M., Taylor, D.I., McNabb, P., Salvitti, L., Ogilvie, S., and Cary, S.C. (2012). Depuration of tetrodotoxin and changes in bacterial communities in *Pleurobranchea maculata* adults and egg masses maintained in captivity. Journal of Chemical Ecology 38, 1342–1350.

Ydenberg, R.C., and Dill, L.M. (1986). The economics of fleeing from predators. Advances in the Study of Behavior 16, 229–249.

Appendix A. Hatching detector transmission script.

```
#include <SPI.h>
#include "RF24.h"


/*************  USER Configuration ****************************/
// Hardware configuration
RF24 radio(8, 7);                       // Set up nRF24L01 radio on SPI bus
plus pins 7 & 8
/************************************************************/


// Function that printf and related will use to print
int serial_putchar(char c, FILE* f) {
  if (c == '\n') serial_putchar('\r', f);
  return Serial.write(c) == 1 ? 0 : 1;
}


FILE serial_stdout;


const uint64_t pipes[2] = { 0xA6CDA3CD71LL, 0x543d52687CLL };   // Radio pipe
addresses for the 2 nodes to communicate.


typedef union sensordata {
  struct {
    byte nodenum;
    byte holder;
    unsigned int mData[6];
    unsigned int sData[6];
    unsigned long int nodeTicks;
    byte xorCheck;
    byte sumCheck;
  } data;

  byte byteseg[32];
};


byte data[32];                          //Data buffer for testing data
transfer speeds


unsigned long counter, rxTimer;         //Counter and timer for keeping
track transfer info
unsigned long startTime, stopTime;
bool TX = 1, RX = 0, role = 0;


void setup(void) {

  Serial.begin(38400);
  pinMode(10, OUTPUT);
  pinMode(9, OUTPUT);
  pinMode(6, OUTPUT);
  pinMode(5, OUTPUT);
  pinMode(4, OUTPUT);
  pinMode(3, OUTPUT);
```

```
    digitalWrite(10, HIGH);
    digitalWrite(9, HIGH);
    digitalWrite(6, HIGH);
    digitalWrite(5, HIGH);
    digitalWrite(4, HIGH);
    digitalWrite(3, HIGH);


    // Select Vref=internal
    ADMUX |= (1 << REFS0)|(1<<REFS1);
    //set prescaller to 64 and enable ADC
    ADCSRA &= ~(1 << ADPS1);
    ADCSRA |= (1 << ADPS2) | (1 << ADPS1) | (1 << ADEN);


    fdev_setup_stream(&serial_stdout, serial_putchar, NULL, _FDEV_SETUP_WRITE);
    stdout = &serial_stdout;


    radio.begin();                              // Setup and configure rf radio
    radio.setChannel(1);
    radio.setPALevel(RF24_PA_MAX);
    radio.setDataRate(RF24_1MBPS);
    radio.setAutoAck(1);                        // Ensure autoACK is enabled
    radio.setRetries(7, 15);                    // Optionally, increase the delay
between retries & # of retries

    radio.setCRCLength(RF24_CRC_8);             // Use 8-bit CRC for performance
    radio.openWritingPipe(pipes[0]);
    radio.openReadingPipe(1, pipes[1]);


    radio.startListening();                     // Start listening
    radio.printDetails();                       // Dump the configuration of the rf
unit for debugging

    radio.powerUp();                            //Power up the radio
}

void loop(void) {

    sensordata sendData;

    sendData.data.nodenum = 1;

    onLED(0);
    delayMicroseconds(200);
    long mvaluea = (long)quadAnalogRead(0) << 13;

    onLED(1);
    delayMicroseconds(200);
    long mvalueb = (long)quadAnalogRead(1) << 13;

    onLED(2);
    delayMicroseconds(200);
    long mvaluec = (long)quadAnalogRead(2) << 13;

    onLED(3);
```

74

```
   delayMicroseconds(200);
   long mvalued = (long)quadAnalogRead(3) << 13;

   onLED(4);
   delayMicroseconds(200);
   long mvaluee = (long)quadAnalogRead(4) << 13;

   onLED(5);
   delayMicroseconds(200);
   long mvaluef = (long)quadAnalogRead(5) << 13;

   long mvalueshift = 0;

   long svaluea = 0;
   long svalueb = 0;
   long svaluec = 0;
   long svalued = 0;
   long svaluee = 0;
   long svaluef = 0;

   long analogVal;
   unsigned long int counter = 0;
   radio.stopListening();

   for (;;) {
     counter++;

     //turn on proper IR LED and turn off old one

     onLED(0);
     delayMicroseconds(200);
     analogVal = (long)quadAnalogRead(0);
     //do the averaging and deviation for the first analog value
     mvalueshift = mvaluea >> 13;
     mvaluea = mvaluea + analogVal - mvalueshift;
     svaluea = svaluea + (analogVal - mvalueshift) * (analogVal - mvalueshift)
- (svaluea >> 13);

     onLED(1);
     delayMicroseconds(200);
     analogVal = (long)quadAnalogRead(1);
     //do the averaging and deviation for the second analog value
     mvalueshift = mvalueb >> 13;
     mvalueb = mvalueb + analogVal - mvalueshift;
     svalueb = svalueb + (analogVal - mvalueshift) * (analogVal - mvalueshift)
- (svalueb >> 13);

     onLED(2);
     delayMicroseconds(200);
     analogVal = (long)quadAnalogRead(2);
     //do the averaging and deviation for the third analog value
     mvalueshift = mvaluec >> 13;
     mvaluec = mvaluec + analogVal - mvalueshift;
     svaluec = svaluec + (analogVal - mvalueshift) * (analogVal - mvalueshift)
- (svaluec >> 13);
```

```
    onLED(3);
    delayMicroseconds(200);
    analogVal = (long)quadAnalogRead(3);
    //do the averaging and deviation for the fourth analog value
    mvalueshift = mvalued >> 13;
    mvalued = mvalued + analogVal - mvalueshift;
    svalued = svalued + (analogVal - mvalueshift) * (analogVal - mvalueshift)
- (svalued >> 13);

    onLED(4);
    delayMicroseconds(200);
    analogVal = (long)quadAnalogRead(4);
    //do the averaging and deviation for the fifth analog value
    mvalueshift = mvaluee >> 13;
    mvaluee = mvaluee + analogVal - mvalueshift;
    svaluee = svaluee + (analogVal - mvalueshift) * (analogVal - mvalueshift)
- (svaluee >> 13);

    onLED(5);
    delayMicroseconds(200);
    analogVal = (long)quadAnalogRead(5);
    //do the averaging and deviation for the sixth analog value
    mvalueshift = mvaluef >> 13;
    mvaluef = mvaluef + analogVal - mvalueshift;
    svaluef = svaluef + (analogVal - mvalueshift) * (analogVal - mvalueshift)
- (svaluef >> 13);

    if (counter == 1000) {
      counter = 0;
      onLED(0);

      delayMicroseconds(200);
      sendData.data.mData[0] = (unsigned int)(mvaluea >> 12);
      sendData.data.sData[0] = (unsigned int)(svaluea >> 13);

      sendData.data.mData[1] = (unsigned int)(mvalueb >> 12);
      sendData.data.sData[1] = (unsigned int)(svalueb >> 13);

      sendData.data.mData[2] = (unsigned int)(mvaluec >> 12);
      sendData.data.sData[2] = (unsigned int)(svaluec >> 13);

      sendData.data.mData[3] = (unsigned int)(mvalued >> 12);
      sendData.data.sData[3] = (unsigned int)(svalued >> 13);

      sendData.data.mData[4] = (unsigned int)(mvaluee >> 12);
      sendData.data.sData[4] = (unsigned int)(svaluee >> 13);

      sendData.data.mData[5] = (unsigned int)(mvaluef >> 12);
      sendData.data.sData[5] = (unsigned int)(svaluef >> 13);

      sendData.data.xorCheck = sendData.byteseg[0] ^ sendData.byteseg[1] ^
sendData.byteseg[2] ^ sendData.byteseg[3] ^ sendData.byteseg[4] ^
sendData.byteseg[5] ^ sendData.byteseg[6] ^ sendData.byteseg[7]
```

76

```
                                    ^ sendData.byteseg[8] ^ sendData.byteseg[9] ^
sendData.byteseg[10] ^ sendData.byteseg[11] ^ sendData.byteseg[12] ^
sendData.byteseg[13] ^ sendData.byteseg[14] ^ sendData.byteseg[15]
                                    ^ sendData.byteseg[16] ^ sendData.byteseg[17]
^ sendData.byteseg[18] ^ sendData.byteseg[19] ^ sendData.byteseg[20] ^
sendData.byteseg[21] ^ sendData.byteseg[22] ^ sendData.byteseg[23]
                                    ^ sendData.byteseg[24] ^ sendData.byteseg[25]
^ sendData.byteseg[26] ^ sendData.byteseg[27] ^ sendData.byteseg[28] ^
sendData.byteseg[29];
      sendData.data.sumCheck = sendData.byteseg[0] + sendData.byteseg[1] +
sendData.byteseg[2] + sendData.byteseg[3] + sendData.byteseg[4] +
sendData.byteseg[5] + sendData.byteseg[6] + sendData.byteseg[7]
                                    + sendData.byteseg[8] + sendData.byteseg[9] +
sendData.byteseg[10] + sendData.byteseg[11] + sendData.byteseg[12] +
sendData.byteseg[13] + sendData.byteseg[14] + sendData.byteseg[15]
                                    + sendData.byteseg[16] + sendData.byteseg[17]
+ sendData.byteseg[18] + sendData.byteseg[19] + sendData.byteseg[20] +
sendData.byteseg[21] + sendData.byteseg[22] + sendData.byteseg[23]
                                    + sendData.byteseg[24] + sendData.byteseg[25]
+ sendData.byteseg[26] + sendData.byteseg[27] + sendData.byteseg[28] +
sendData.byteseg[29];
      radio.writeFast(sendData.byteseg, 32);
      radio.txStandBy();


    }
  }
}


unsigned int quadAnalogRead(byte channel) {
  unsigned int analogVal;

  ADMUX = (ADMUX & 0xF0) | (channel);  //0b00000000 for ch 0, 0b00000001 for
ch 1, etc.
  //single conversion mode
  ADCSRA |= (1 << ADSC);
  // wait until ADC conversion is complete
  while ( ADCSRA & (1 << ADSC) );
  analogVal = ADC;

  ADCSRA |= (1 << ADSC);
  // wait until ADC conversion is complete
  while ( ADCSRA & (1 << ADSC) );
  analogVal += ADC;

  ADCSRA |= (1 << ADSC);
  // wait until ADC conversion is complete
  while ( ADCSRA & (1 << ADSC) );
  analogVal += ADC;

  ADCSRA |= (1 << ADSC);
  // wait until ADC conversion is complete
  while ( ADCSRA & (1 << ADSC) );
  analogVal += ADC;
}
```

```
void onLED(byte ledNum){
  digitalWrite(10, HIGH);
  digitalWrite(9, HIGH);
  digitalWrite(6, HIGH);
  digitalWrite(5, HIGH);
  digitalWrite(4, HIGH);
  digitalWrite(3, HIGH);

  switch(ledNum){
    case 0:
      digitalWrite(10, LOW);
      break;
    case 1:
      digitalWrite(9, LOW);
      break;
    case 2:
      digitalWrite(6, LOW);
      break;
    case 3:
      digitalWrite(5, LOW);
      break;
    case 4:
      digitalWrite(3, LOW);
      break;
    case 5:
      digitalWrite(4, LOW);
      break;
    default:
      break;
  }

  return;
}
```

Appendix B. Hatching detector receiver script.

```
#include <SPI.h>
#include "RF24.h"

/************* USER Configuration ****************************/
// Hardware configuration
RF24 radio(8, 7);                        // Set up nRF24L01 radio on SPI bus
plus pins 7 & 8

/***********************************************************/

// Function that printf and related will use to print
int serial_putchar(char c, FILE* f) {
  if (c == '\n') serial_putchar('\r', f);
  return Serial.write(c) == 1 ? 0 : 1;
}

FILE serial_stdout;

const uint64_t pipes[2] = { 0x543d52687CLL, 0xA6CDA3CD71LL  };   // Radio
pipe addresses for the 2 nodes to communicate.

typedef union sensordata {
  struct {
    byte nodenum;
    byte holder;
    unsigned int mData[6];
    unsigned int sData[6];
    unsigned long int nodeTicks;
    byte xorCheck;
    byte sumCheck;
  } data;

  byte byteseg[32];
};

byte data[32];                           //Data buffer for testing data
transfer speeds

unsigned long counter, rxTimer;          //Counter and timer for keeping
track transfer info
unsigned long startTime, stopTime;
bool TX = 1, RX = 0, role = 0;

void setup(void) {

  Serial.begin(38400);

  fdev_setup_stream(&serial_stdout, serial_putchar, NULL, _FDEV_SETUP_WRITE);
  stdout = &serial_stdout;

  radio.begin();                         // Setup and configure rf radio
  radio.setChannel(1);
  radio.setPALevel(RF24_PA_MAX);
  radio.setDataRate(RF24_1MBPS);
```

```
  radio.setAutoAck(1);                       // Ensure autoACK is enabled
  radio.setRetries(7, 15);                   // Optionally, increase the delay
between retries & # of retries

  radio.setCRCLength(RF24_CRC_8);            // Use 8-bit CRC for performance
  radio.openWritingPipe(pipes[0]);
  radio.openReadingPipe(1, pipes[1]);

  radio.startListening();                    // Start listening
  radio.printDetails();                      // Dump the configuration of the rf
unit for debugging


  radio.powerUp();                           //Power up the radio
}

void loop(void) {

  sensordata receivedData;


  while (radio.available()) {
    radio.read(&receivedData, 32);
    if ((receivedData.data.xorCheck == receivedData.byteseg[0] ^
receivedData.byteseg[1] ^ receivedData.byteseg[2] ^ receivedData.byteseg[3] ^
receivedData.byteseg[4] ^ receivedData.byteseg[5] ^ receivedData.byteseg[6] ^
receivedData.byteseg[7]
        ^ receivedData.byteseg[8] ^ receivedData.byteseg[9] ^
receivedData.byteseg[10] ^ receivedData.byteseg[11] ^
receivedData.byteseg[12] ^ receivedData.byteseg[13] ^
receivedData.byteseg[14] ^ receivedData.byteseg[15]
        ^ receivedData.byteseg[16] ^ receivedData.byteseg[17] ^
receivedData.byteseg[18] ^ receivedData.byteseg[19] ^
receivedData.byteseg[20] ^ receivedData.byteseg[21] ^
receivedData.byteseg[22] ^ receivedData.byteseg[23]
        ^ receivedData.byteseg[24] ^ receivedData.byteseg[25] ^
receivedData.byteseg[26] ^ receivedData.byteseg[27] ^
receivedData.byteseg[28] ^ receivedData.byteseg[29]) &&
        (receivedData.data.sumCheck == (byte)(receivedData.byteseg[0] +
receivedData.byteseg[1] + receivedData.byteseg[2] + receivedData.byteseg[3] +
receivedData.byteseg[4] + receivedData.byteseg[5] + receivedData.byteseg[6] +
receivedData.byteseg[7]
        + receivedData.byteseg[8] + receivedData.byteseg[9] +
receivedData.byteseg[10] + receivedData.byteseg[11] +
receivedData.byteseg[12] + receivedData.byteseg[13] +
receivedData.byteseg[14] + receivedData.byteseg[15]
        + receivedData.byteseg[16] + receivedData.byteseg[17] +
receivedData.byteseg[18] + receivedData.byteseg[19] +
receivedData.byteseg[20] + receivedData.byteseg[21] +
receivedData.byteseg[22] + receivedData.byteseg[23]
        + receivedData.byteseg[24] + receivedData.byteseg[25] +
receivedData.byteseg[26] + receivedData.byteseg[27] +
receivedData.byteseg[28] + receivedData.byteseg[29]))) {
      Serial.print(receivedData.data.nodenum);
      Serial.print('\t');
      Serial.print(receivedData.data.mData[0]);
      Serial.print('\t');
```

```
        Serial.print(receivedData.data.sData[0]);
        Serial.print('\t');
        Serial.print(receivedData.data.mData[1]);
        Serial.print('\t');
        Serial.print(receivedData.data.sData[1]);
        Serial.print('\t');
        Serial.print(receivedData.data.mData[2]);
        Serial.print('\t');
        Serial.print(receivedData.data.sData[2]);
        Serial.print('\t');
        Serial.print(receivedData.data.mData[3]);
        Serial.print('\t');
        Serial.print(receivedData.data.sData[3]);
        Serial.print('\t');
        Serial.print(receivedData.data.mData[4]);
        Serial.print('\t');
        Serial.print(receivedData.data.sData[4]);
        Serial.print('\t');
        Serial.print(receivedData.data.mData[5]);
        Serial.print('\t');
        Serial.println(receivedData.data.sData[5]);
    } /*else{
        Serial.println("CHECKSUM FAILED!");
        Serial.println(receivedData.data.xorCheck);
        Serial.println(receivedData.byteseg[0] ^ receivedData.byteseg[1] ^
receivedData.byteseg[2] ^ receivedData.byteseg[3] ^ receivedData.byteseg[4] ^
receivedData.byteseg[5] ^ receivedData.byteseg[6] ^ receivedData.byteseg[7]
        ^ receivedData.byteseg[8] ^ receivedData.byteseg[9] ^
receivedData.byteseg[10] ^ receivedData.byteseg[11] ^
receivedData.byteseg[12] ^ receivedData.byteseg[13] ^
receivedData.byteseg[14] ^ receivedData.byteseg[15]
        ^ receivedData.byteseg[16] ^ receivedData.byteseg[17] ^
receivedData.byteseg[18] ^ receivedData.byteseg[19] ^
receivedData.byteseg[20] ^ receivedData.byteseg[21] ^
receivedData.byteseg[22] ^ receivedData.byteseg[23]
        ^ receivedData.byteseg[24] ^ receivedData.byteseg[25] ^
receivedData.byteseg[26] ^ receivedData.byteseg[27] ^
receivedData.byteseg[28] ^ receivedData.byteseg[29]);
        Serial.println(receivedData.data.sumCheck);
        Serial.println(receivedData.byteseg[0] + receivedData.byteseg[1] +
receivedData.byteseg[2] + receivedData.byteseg[3] + receivedData.byteseg[4] +
receivedData.byteseg[5] + receivedData.byteseg[6] + receivedData.byteseg[7]
        + receivedData.byteseg[8] + receivedData.byteseg[9] +
receivedData.byteseg[10] + receivedData.byteseg[11] +
receivedData.byteseg[12] + receivedData.byteseg[13] +
receivedData.byteseg[14] + receivedData.byteseg[15]
        + receivedData.byteseg[16] + receivedData.byteseg[17] +
receivedData.byteseg[18] + receivedData.byteseg[19] +
receivedData.byteseg[20] + receivedData.byteseg[21] +
receivedData.byteseg[22] + receivedData.byteseg[23]
        + receivedData.byteseg[24] + receivedData.byteseg[25] +
receivedData.byteseg[26] + receivedData.byteseg[27] +
receivedData.byteseg[28] + receivedData.byteseg[29]);
    }*/

  }
}
```

Appendix C. R script for quasi-real time hatch monitoring.

```
library(data.table)                    # data wrangling
library(ggplot2)                       # plotting
library(ggpubr)                        # easily combine plots with common legend

# Set working directory to raw data folder

# Set theme for plots
theme_set(
  theme_gray() +
    theme(
      text = element_text(family = "Times"),
      panel.background = element_blank(),
      axis.line = element_line(color="black"),
      axis.text.x = element_text(color="black")
    )
)


#==============#
# MULTIPLOT ####
#==============#

# 'multiplot()' plots hatching observations from a specified .txt file. It is
# used for quasi-real-time monitoring of hatching activity and identifying
# malfunctioning IR emitter-phototransistor sensors.

multiplot <- function(file, measure = "var", size = 1e3) {

  if(is.numeric(file)) file <- list.files()[file]

  # Specify name of .txt file to load and format
  dat <- suppressWarnings(fread(file, sep="\t", header=F, fill=T))
  dat <- dat[complete.cases(dat)]
  dat$V1 <- as.POSIXct(dat$V1)
  setnames(dat,
    c("Date", "Sensor", paste0(rep(c("m", "v"), times=6), rep(1:6, each=2)))
  )

  # Melt data to longform, then sort data by sensor and date. Omit NAs.
  dat_melt <- melt(dat,
   id.vars=c("Date", "Sensor"), measure.vars= patterns("m", "v"),
   value.name=c("mean", "var"), variable.name="LED"
  )
  setkey(dat_melt, Sensor, LED, Date)
  dat_melt <- dat_melt[!(is.na(mean))]

  # Trim down datasets
  dat_split <- split(dat_melt, by="Sensor")
  dat_plot <- rbindlist(
      mapply(
      FUN = function(x,y) {x[seq(from=1, to=y[1], by=y[2])]},
      x = dat_split,
      y = lapply(dat_split, function(x) {
        c(nrow(x), floor(nrow(x) / ifelse(nrow(x)>size*5, size, 1)))}
      ),
```

```r
      SIMPLIFY = F
    )
  )
  setnames(dat_plot, old=measure, new="value")
  setkey(dat_plot, Sensor, LED, Date)

  # Set plot styles
  plot_styles <- list(
    facet_wrap(~Sensor, scales="free_y"),
    geom_point(aes(x=Date, y=value, color=LED), size=0.5, shape=1),
    scale_color_manual(values=grey.colors(n=6)),
    scale_x_datetime(
      date_breaks = c("1 day"),
      date_labels = c("%b-%d"),
      date_minor_breaks = c("6 hours")
    ),
    theme(
      axis.text.x = element_text(angle=90, hjust=1, vjust=0.5),
      strip.text.x = element_text(margin=margin(2,0,2,0))
    )
  )

  # Plot
  ggplot(dat_plot) + plot_styles +labs(y="Running deviation of IR intensity")
}

### Examples ###
# multiplot(20)                                   # Specify file index
# multiplot("2017-11-14_HC_1.txt")                # Or file name
directly
# multiplot("2017-11-14_HC_1.txt", measure="mean")     # plot means if
specified

#=========#
# ZOOM ####
#=========#

# The 'zoom()' function is used to visualize the entire time series for a
# specified sensor. Specify index of files to plot, as sensors may be used
for
# multiple replicates.

zoom <- function(sensor, from, to, size=1e4) {
  # sensor <- 36; from <-  5; to <- 22; size <- 1e4
  # sensor <-  1; from <- 12; to <- 28; size <- 1e4

  # Identify and load files, subset by sensor, and stitch together
  filenames <- list.files()[from:to]
  dat <- rbindlist(
    lapply(filenames, function(x) {
      d <- suppressWarnings(fread(x, sep="\t", header=F, fill=T))[V2==sensor]
      d <- d[complete.cases(d)]
      d$V1 <- as.POSIXct(d$V1)
      d
    })
  )
  setnames(dat,
```

```r
    c("Date", "Sensor", paste0(rep(c("m", "v"), times=6), rep(1:6, each=2)))
  )
  setkey(dat, Sensor, Date)

  # Reduce data to manageable size
  dat <- dat[seq(from=1, to=.N, by=.N/size) ]

  # Melt to longform
  dat_melt <- melt(dat, id.vars=c("Date", "Sensor"))
  dat_melt[, LED := gsub("[a-z]", "", variable)]
  dat_melt[, measure := gsub("[0-9]", "", variable)]
  setkey(dat_melt, Sensor, measure, LED)

  # Set plot styles
  plot_styles <- list(
    geom_point(aes(x=Date, y=value, color=LED), size=1, stroke=0.25),
    scale_color_manual(values=grey.colors(n=6)),
    scale_x_datetime(
      date_breaks = c("1 day"),
      date_labels = c("%b-%d")),
    theme(
      axis.text.x = element_text(angle=45, hjust=1, vjust=1),
      strip.text.x = element_blank(),
      strip.background.x = element_blank(),
      strip.background.y = element_blank(), strip.text.y. = element_blank()
    )
  )

  # Plot
  mean_plot <- ggplot(dat_melt[measure=="m"]) + plot_styles +
    labs(subtitle="Mean") + facet_grid(Sensor~"")
  var_plot <- ggplot(dat_melt[measure=="v"]) + plot_styles +
    labs(subtitle="Variance") + facet_grid(LED~"", scales="free_y")
  ggarrange(
    mean_plot + rremove("x.title") + rremove("x.text"),
    var_plot, common.legend = T,
    heights=c(0.3, 0.7), ncol=1, legend = "right", align="v")
}

### Examples ###
# zoom(sensor=11, from=26, to=42)   # Undisturbed hatching (order 50)
# zoom(sensor=28, from=33, to=47)   # induced hatching from attack (order 66)


#==================#
# Plots for Ch 2 ####
#==================#
# Quasi-real-time hatch monitoring
ggsave(
  plot = multiplot(20),
  filename = "/Users/Geoff/Desktop/Thesis
Research/THESIS/Figures/hatch_monitoring.png",
  width=9, height=5, units="in", dpi=300
)

# Example of raw data from control and attack treatments
ggsave(
```

```
  plot = ggarrange(
    annotate_figure(zoom(sensor=11, from=26, to=42), fig.lab="A"),
    annotate_figure(zoom(sensor=28, from=33, to=47), fig.lab="B"),
    ncol=2
  ),
  filename = "/Users/Geoff/Desktop/Thesis
Research/THESIS/Figures/hatch_example.png",
  width=9, height=5, units="in", dpi=300
)
```

Appendix D. R script for denoising and simplifying raw hatching detector data and performing breakpoint analysis to determine hatch timing.

```
hatch_timing <- function(data, t1=12, t2=0, l=3, brk_n=1, rho=0.05, M=200,
q=0.9995, ci=0.9999, win=15){

  # calculate the population variance (i.e. without n-1 correction)
  sd_fun <- function(x){
    z <- x[!is.na(x)]
    sqrt(sum((z-mean(z))^2)/length(z))
  }

  # Load up data and remove faulty sensors and all mean data.
  x0 <- readRDS(paste("HC_Experiment_Data/HC_rds/HC", data, ".rds", sep=""))
  dat_name <- unique(x0$Order)

  # sensors to mute
  mute <- paste("sd", mute_list[con==unique(x0$Order), sen], sep="")
  # Pull embryo mass oviposition date and if present, attack date
  depo_datetime <- dat_sum[Order == unique(x0$Order), Deposition.date]
  phys_datetime <- dat_sum[Order == unique(x0$Order), Phys80.date]

  x1 <- x0[, -(grep("^mean", names(x0))), with=FALSE]      # remove mean data
  x2 <- melt(x1, id.vars=c("DateTime", "Container", "Order")) # melt
  x3 <- x2[!(variable %in% mute)]                            # omit muted sensors
  x4 <- x3[DateTime > min(DateTime) + hours(t1) &
           DateTime < max(DateTime) - hours(t2)] # Trim off hours from ends

  # remove outliers here so they aren't folded in to the 3-min mean/sd!
  qua <- x4[, .(quant = quantile(value, q)), by=variable]

  # Scale values within sensors so mean=0 and sd=1
  x4[, quant := qua[x4, quant, on="variable"]]
  x4[, value_q := ifelse(value > quant, NA, value)]
  x4[, value_r := scale(value_q, center=FALSE), by=variable]

  # calculate mean and population sd for each 3-minute interval
  window <- l*60   # l is in minutes, so multiply by 60 seconds
  intervals <- seq(
    from=trunc(min(x1[, DateTime]), units="hours"),
    to=round(max(x1[, DateTime]), units="hours")+hours(1),
    by=window)
  x4[, CUT := cut(x4[, DateTime], breaks=intervals)]
  x5 <- x4[, .(
    N=.N,
    mean=mean(value_r, na.rm=TRUE),
    se=sd_fun(value_r)),
    by=.(variable, CUT) ]
  x5[, INDEX := .SD[, .I], by=variable]

  # if some cuts have all data values counted as outliers, take running mean
  x5[, mean := ifelse(is.na(mean), runmean(mean, k=15), mean)]
  x5[, se   := ifelse(is.na(se), runmean(se, k=15), se)]

  # calculate cumulative mean/se for each sensor
  # Use this to scale the curves from each sensor to have the same area
```

```
x5[, ':=' (mean_c = cumsum(mean), se_c = cumsum(se)), by=variable]
# calculate total area of cmsm curve
mean_c_t <- x5[, .(ttl_cmsm= caTools::trapz(INDEX, mean_c)), by=variable]
mean_c_t[, cmsm_s := ttl_cmsm/max(ttl_cmsm)]
# calculate total area of cmsm curve
se_c_t <- x5[, .(ttl_cmsm= caTools::trapz(INDEX, se_c)), by=variable]
se_c_t[, cmsm_s := ttl_cmsm/max(ttl_cmsm)]

# adjust each cmsm curve to have the same area
x5[, mean_s := mean_c_t[x5, cmsm_s, on="variable"]]
x5[, se_s := se_c_t[x5, cmsm_s, on="variable"]]
x5[, mean_scale := mean/mean_s]
x5[, se_scale := se/se_s]

# Determine the maximum AUC
y_max <- quantile(x5$se_scale, 0.99)

# mmm() is 'mean minus max', which excludes the maximum value from the
# sensors at a given time point before calculating the mean
# This helps remove outliers (if one sensor doesn't agree with others), but
# if two sensors see something, the 2nd highest will still pull mean up
mmm_fun <- function(x){
  y <- max(x)
  (sum(x)-y) / (length(x)-1)
}

x6 <- x5[, .(
  se_value = mmm_fun(se_scale),
  mean_value = mmm_fun(mean_scale)),
  by=.(INDEX, CUT)]

# If data is still noisy, do another round of outlier removal
if(!is.null(ci)){
  x6[, ci_u := x6[
    INDEX >= (as.numeric(.BY[1]) - win) & INDEX <=(as.numeric(.BY[1])+win),
    t.test(se_value, conf.level=ci)$conf.int[2]],
    by=.(INDEX)]
  x6[, chk := se_value > ci_u , by=.(INDEX)]
  x6 <- x6[chk==FALSE] # keep only values less than the upper CI
}

# calculate running mean of se_value, merging all sensors into one signal
x6[, r_s := runmean(se_value, k=win)]

# Identify the breakpoint
r_s_b <- CE.Normal.MeanVar(x6[, .(r_s)], Nmax=brk_n)$BP.Loc
r_s_c <- round(
  as.numeric(as.POSIXct(x6[r_s_b, CUT]) - depo_datetime, "days"),2)
r_s_d <- x6[r_s_b, INDEX]

# if breakpoint is < 7.05, rerun with trimmed dataset
if(brk_n==1){
  if(r_s_c < 7.05){
    message(paste(
      "Originally found ", r_s_c, ". Rerunning after age=7...", sep=""))

    # Cut that corresponds to age=7
```

```
      c7 <- findInterval(depo_datetime + days(7), as.POSIXct(unique(x5$CUT)))
      x7 <- x6[INDEX > c7]
      r_s_b2 <- CE.Normal.MeanVar(x7[, .(r_s)], Nmax=1)$BP.Loc + c7
      r_s_b <- c(r_s_b, r_s_b2)
      r_s_d <- c(r_s_d, x6[r_s_b2, INDEX])
      r_s_c <- c(r_s_c, round(
        as.numeric(as.POSIXct(x6[r_s_b2, CUT]) - depo_datetime, "days"),2))
    }
  }

  hatch_time <- geom_vline(
    xintercept=r_s_d[1],
    color="black", linetype=2, size=0.5, alpha=0.75
  )
  a <- ggplot(x5, aes(x=INDEX, y=se_scale, color=variable)) +
    geom_point(size=0.5, alpha=0.25, na.rm=TRUE) +
    scale_color_manual(values = grey.colors(n=6)) +
    scale_y_continuous(limits=c(0, y_max)) + hatch_time +
    theme(
      legend.position = "none", axis.text.y=element_text(angle=90,hjust=0.5),
      axis.text.x=element_blank(),
     axis.text.y=element_text(angle=90, hjust=0.5)) + rremove("x.title")
    ) +
    labs(
      y="SE scaled",
      subtitle=paste(
        "HC", data, "Hatch_Age:",
        paste(r_s_c[1], collapse=", "), sep=" ")
    )
  b <- ggplot(x6, aes(x=INDEX, y=se_value)) + geom_line(color="gray60") +
    hatch_time +
    theme(
      axis.text.x=element_blank(),
      axis.text.y=element_text(angle=90, hjust=0.5)
    ) + rremove("x.title") + labs(y="Mean (excl. max)")
  c <- ggplot(x6, aes(x=INDEX, y=r_s)) + geom_line(color="gray60") +
    hatch_time + labs(y="Final")

  print(noquote(paste(
    "Estimated age at hatching: ", paste(r_s_c, collapse=", "), sep="")) 
  )

  return(
    ggarrange(
      a, b, c,
      ncol=1, heights = c(0.35, 0.3, 0.35), align="v")
  )
}
```